COMPARATIVE CHEMICAL ECOLOGY OF INVASIVE *DEPRESSARIA* SPECIES (LEPIDOPTERA: DEPRESSARIIDAE) VARYING IN HOSTPLANT SPECIFICITY

BY

CHARLES-ANTOINE EDOUARD DEAN

DISSERTATION

Submitted in partial fulfillment of the requirements
for the degree of Doctor of Philosophy in Entomology
in the Graduate College of the
University of Illinois at Urbana-Champaign, 2022

Urbana, Illinois

Doctoral Committee:

Professor May R. Berenbaum, Chair and Director of Research
Professor James B. Whitfield
Assistant Professor Adam G. Dolezal
Dr. Bernarda Calla

ABSTRACT

The purple carrot seed moth (*Depressaria depressana*) (Fabricius) (Lepidoptera: Depressariidae) is a newly invasive species in North America. This moth is of Eurasian origin and, unlike its well-studied congener the parsnip webworm (*Depressaria radiella*), it is a family-level specialist of the Apiaceae, utilizing more than a dozen species in multiple tribes within the family. By contrast, *D. radiella* is a superspecialist that feeds almost exclusively on species in the genera *Pastinaca* and *Heracleum* in Europe and in areas of introduction around the world. The presence of *D. depressana* in North America offers a unique opportunity to study the evolutionary and ecological mechanisms underlying the adaptation of a family specialist to a novel environment during the early stages of its colonization. Such an investigation can not only reveal the similarities and differences between biological invaders of divergent feeding strategies but can also provide insight into the dynamics of plant-insect interactions involving an introduced family specialist and chemically defended hosts that can provide a framework for management strategies for future invasive species that fill a similar ecological niche.

In the first chapter of my dissertation, I investigated whether differences in furanocoumarin metabolism exist between *D. depressana* and two isolated populations of *D. radiella* feeding exclusively on either *P. sativa* or *H. maximum*. I also compared four gravimetric estimates of efficiency to assess *D. depressana* larval performance on different diets. Both populations of *D. radiella* metabolized furanocoumarins at a greater rate than *D. depressana*. Although there was no difference in rates of metabolism of linear furanocoumarins in the two populations of *D. radiella*, individuals collected from *H. maximum* metabolized angular furanocoumarins more rapidly. The gravimetric assessments of performance revealed that *D.*

depressana exhibited highest efficiencies of conversion of ingested food when consuming *D. carota*; moreover, this species could survive consuming fruits of *Zizia aurea*, an apiaceous species native to North America. Lastly, I performed a preliminary phylogenetic analysis, building on an earlier analysis based on morphological characters, by adding data from the mitochondrial cytochrome oxidase subunit 1 (COI) barcoding gene. Results indicate that adaptation to furanocoumarins is not a strong predictor of species-level evolution in *Depressaria*.

In the second chapter of my dissertation, I evaluated differences in physiological mechanisms of adaptation to phototoxic furanocoumarins in the two species of *Depressaria.* Earlier work revealed that *D. radiella* sequesters lutein, a carotenoid pigment, in response to UV light exposure and dietary furanocoumarins, apparently as a mechanism to reduce phototoxicity. Accordingly, I examined differences in expression of the *ninaB* gene in response to dietary β-carotene, xanthotoxin, and B-carotene + xanthotoxin among *D. radiella*, a superspecialist feeder, *D. depressana*, a family-level specialist, and *Trichoplusia ni*, a broadly polyphagous herbivore. The ninaB enzyme is involved in the cleavage of carotenoids, which are pigments that aid in a broad array of biological functions, including ultraviolet light protection, vision, color pattern development, and antioxidant defenses. I found that, in all three species, *ninaB* is significantly downregulated across all three experimental diets relative to the unamended artificial diet control. However, there was no consistent pattern within each species across treatments. These results indicate that cleavage of B-carotene is downregulated in the presence of dietary furanocoumarins, but whether sequestration of unmodified β-carotene either directly reduces toxicity of furanocoumarins or enhances the activity of detoxifying cytochrome P450 monooxygenase enzymes remains an open question.

For the third chapter of my dissertation, I characterized the CYPome, or complete inventory of genes encoding cytochrome P450 monooxygenases, the principal Phase 1 detoxification enzymes utilized by most lepidopterans, in the *D. depressana* genome and evaluated the transcriptomic response of *D. depressana* to consumption of the linear furanocoumarin xanthotoxin and the angular furanocoumarin sphondin. The cytochrome P450 monooxygenases (P450s) involved in metabolism mediate detoxification of xenobiotics, including furanocoumarins, by catalyzing oxidation reactions whereby oxygen is added to lipophilic compounds to increase water solubility and excretion from the cell. In many specialist herbivores, detoxifying P450s have become highly specialized over evolutionary time and differences in susceptibility to furanocoumarins can potentially be explained by a diversity of P450s with narrow substrate specificities. I found that the *D. depressana* CYPome encompasses 76 P450 genes, including 7 Clan 2, 37 Clan 3, 24 Clan 4, and 11 mitochondrial clan P450s. This CYPome is the smallest of the seven lepidopteran species considered in this analysis. Transcriptomic responses to dietary xanthotoxin revealed striking widespread differential expression relative to the sphondin and control treatments. A Gene Ontology (GO) enrichment analysis revealed that upregulation was highest among genes involving DNA replication, transcription, and metabolic processes. The transcriptomic response to dietary sphondin was virtually nonexistent and a GO enrichment analysis was not conducted.

For my fourth chapter, I assessed the genetic structure of invasive *D. depressana* populations across latitudinal and longitudinal gradients in the eastern United States by constructing haplotype networks using the mitochondrial COI and nuclear EF1α markers. This experiment allowed me to assess interpopulational diversity and gene flow across 301 individuals from 17 populations collected in 7 states. In my analysis, both markers exhibited high

genetic diversity, which indicates high levels of gene flow, or, given the recency of its introduction, insufficient evolutionary time for localized adaptation to occur among populations of *D. depressana*. In the case of COI, few haplotypes were recovered and comparisons to European and Canadian populations did not reveal a likely source population. Conversely, many EF1α haplotypes were recovered in this experiment, which obscured any evaluation of dispersal routes across the continent. Geographic features, such as rivers and mountains, did not appear to obstruct gene flow across populations.

Together my chapters provide a novel aspect to the plant-insect coevolutionary model first established by the parsnip webworm and wild parsnip system. As a newly invasive congener of the parsnip webworm, *D. depressana* maintains a greater diet breadth as a family-level specialist and therefore serves as a point of comparison to the superspecialist, *D. radiella*. My chapters examine the reciprocal selective pressure between plant phytochemistry and herbivore detoxification by broadening the understanding of the role that diet breath plays in the dynamics underlying invasion biology.

ACKNOWLEDGMENTS

I would like to begin by extending my deepest gratitude to my advisor, Dr. May Berenbaum. She has provided me with so many invaluable opportunities, support, and professional advice. She made graduate school fun and her wealth of experience and knowledge have always inspired me to be the best scientist I can be. Next, I would like to thank Dr. Bernarda Calla for her significant contributions to my research and her infinite patience with me as I learn the ropes of transcriptomics. I would also like to thank my remaining committee members, Dr. James Whitfield and Dr. Adam Dolezal, whose input has truly elevated the quality of my research. I would like to thank Dr. Aron Katz, who very graciously lent his expertise in the field of insect systematics to make the *Depressaria* phylogeny possible in Chapter 1 of this thesis. I would also like to thank Dr. Terry Harrison, who helped me first identify *D. depressana* back in 2015 – the species that would eventually become the basis of every chapter in my dissertation. I thank all Berenbaum lab members that I had the good fortunate of working with over the years: Teresia Njoroge, Daniel Pearlstein, Jake Dixon, Will Montag, Ed Hsieh, Mark Demkovich, Daniel Bush, Wen Yen Wu, and Ling-Hsiu Lao. In particular, I would like to express my appreciation for Ling-Hsiu and Wen Yen, who helped me learn midgut dissections/bioassays and HPLC - skills necessary for the completion of Chapter 1. I also thank Jack Easley, an undergraduate researcher who worked tirelessly both in the field and at? the lab bench to help me collect the necessary data for Chapter 4. I would like to thank the amazing staff in the UIUC Entomology department office, Kim Leigh and Liz Barnabe, for helping me stay on track, as well as Karl Schlipf and Jeff Haas in the IT department for saving my data files more times than I can count. Thank you to all my friends in the Entomology

department: Aron Katz, Rafa Achury-Morales, Mark Demkovich, Tom Schmeelk, Jon Tetlie, Scott Clem, Ed Hsieh, Josh Gibson, and Jake Dixon for giving me so many great memories and making my experience in Illinois truly unforgettable. Lastly, I thank my family--my mother, Marisa Dean, my father Donald Dean, my younger brother Francois Dean, and my older brother Sam Dean, and his family Kat, Lily, Evaline, and Ollie--for their support over the years as I followed my dream.

This dissertation is dedicated to my wonderful mother and father, Marisa and Donald Dean, without whom I could not have completed my degree. Their constant love and support were invaluable and continue to inspire me.

TABLE OF CONTENTS

CHAPTER 1

DEGREE OF DIETARY SPECIALIZATION ON FURANOCOUMARIN-CONTAINING HOSTPLANTS IN A NEWLY INVASIVE SPECIES, *DEPRESSARIA DEPRESSANA* (LEPIDOPTERA: DEPRESSARIIDAE)

INTRODUCTION

Adaptive radiation is defined as the process in which ancestral species diversify into many new forms in response to environmental changes that create new habitats, make new resources available, or alter interactions with other species. This process underlies the seminal "escape and radiation" hypothesis outlined by Ehrlich and Raven (1964) to account for hostplant association patterns across a broad range of butterflies encompassing five families. In this model, Ehrlich and Raven (1964) proposed that plant lineages enter new adaptive zones within which they are free to diversify rapidly after escaping selective pressures of herbivory through novel defensive adaptations. Insects that subsequently evolve suitable counter-adaptations to these defenses are provided with a new exploitable food resource and thus similarly undergo rapid diversification upon entering an adaptive zone of their own. This "arms race" of key innovations resulting in escalating reciprocal selective pressure within plant-insect interactions is thought to be a driving force underlying the evolution of specialist feeding strategies in insects (Berenbaum et al. 1996).

In terms of degrees of specialization of herbivorous insects, Ali and Agrawal (2019) defined insects that feed on only a single plant taxon and its close relatives (often within one genus) as monophagous, on several genera (often within a single family) as oligophagous, and on more than one plant family as polyphagous, or "highly generalized." However, these authors

note, “The distribution of feeding on one plant species to a diversity of plants is truly a graded continuum.” Even within groups of herbivores conventionally defined as specialists, a continuum of feeding strategies can exist, with some family-level specialists feeding on hostplants on multiple tribes within a family and other family-level specialists restricted to only one or two closely related genera. Thus, family-specialists, which feed broadly across a hostplant family, can potentially encounter a more diverse array of defense chemicals than would family-specialists restricted to a small number of closely related genera with similar phytochemical profiles, i.e., "super-specialists," and may consequently differ in the degree of specialization of their detoxification mechanisms. Diet breadth, even within a single hostplant family, may provide insights into the likelihood of success of a specialist group in invading new habitats and colonizing novel hostplants.

The insect herbivore community of species in the family Apiaceae is dominated by specialists, a pattern thought to reflect the toxicological challenges presented by the defensive chemistry of the family (Berenbaum 1990). Among the widely distributed defensive phytochemicals in the family are furanocoumarins, which owe their broad toxicity to their ability to bind to DNA in the presence of ultraviolet light and interfere with transcription (Berenbaum 1991). Studies of the changes in furanocoumarin structure and composition throughout the evolutionary history of Apiaceae, as well as the subsequent evolution of furanocoumarin resistance in species in the genus *Papilio* (Lepidoptera: Papilionidae), provided early evidence suggestive of the mechanisms underlying the steps involved in the “escape and radiate” model (Berenbaum 1983). Of the two main structural classes of furanocoumarins, characterized by the attachment of the furan ring to the coumarin nucleus, linear furanocoumarins are widely distributed across four plant families and sporadically in seven additional families, whereas

angular furanocoumarins are more derived and restricted in distribution, effectively limited to only a handful of genera in three families (Berenbaum 1991; Bruni et al. 2019).

Among Apiaceae specialists are the majority of species in the genus *Depressaria* with known feeding habits (Bucheli et al. 2010). The genus is Holarctic in distribution, with approximately 100 described species; Passoa (1995) and Bucheli et al. (2010) suggested that the Apiaceae is the ancestral host family, with the association likely originating in the Palearctic with “multiple colonization events into the Nearctic region" (Bucheli et al. 2010). Within the genus, however, there is a range of variation in the degree of specialization; whereas some species feed broadly on species in multiple tribes within the family (or in some cases, on species in the Asteraceae or Rutaceae), others are restricted to only one or two closely related genera within a single tribe (Table 1).

In lepidopterans specialized to some extent on apiaceous hostplants, furanocoumarins are metabolized largely via cytochrome P450 monooxygenases (Berenbaum et al. 1986; Mao et al. 2006; Calla et al. 2020). A long-studied Apiaceae-specialist is the parsnip webworm, *Depressaria radiella* (formerly *D. pastinacella*), a Eurasian species that was first introduced to North America in the mid-19th century (Zangerl and Berenbaum 2003). As a specialist with few hostplants other than species in the closely allied genera *Pastinaca* and *Heracleum, D. radiella* displays phenotype matching with its principal eastern North American hostplant *Pastinaca sativa* (wild parsnip), whereby population-level profiles of furanocoumarin detoxification activity reflect the population-level profile of furanocoumarin defensive chemistry of the immature fruits of its hostplants (Berenbaum and Zangerl 1992). Since its introduction to North America, *D. radiella* has colonized the native species *Heracleum maximum* (cow parsnip) (Zangerl and Berenbaum 2003), a congener of several European hostplant species, including *H.*

sphondylium and *H. sibiricum* (Palm 1989). Relative to *P. sativa*, and to most other apiaceous species in other genera, *H. maximum* produces a broad spectrum of furanocoumarins, including six angular furanocoumarins (Berenbaum 1981; O'Neill et al. 2013; Dhar et al. 2014). In one central Illinois population, levels of sphondin, an angular furanocoumarin commonly produced by apiaceous species, in *H. maximum* were 29-fold higher than levels in nearby populations of *P. sativa* (Berenbaum and Zangerl 1991). Although a comparison of performance of *D. radiella* on these two hostplants revealed overall higher survival of larvae on *P. sativa* irrespective of their natal hostplant, Berenbaum and Zangerl (1991) found that larvae from *H. maximum* populations exhibited more rapid development and higher pupal weights on diets containing fruits of *H. maximum* compared to individuals collected from *P. sativa* and raised on the same diet (Berenbaum and Zangerl 1991), suggestive of some degree of local adaptation.

Less is known about the furanocoumarin detoxification capacity of a *D. radiella* congener, the recently invasive *Depressaria depressana*. This exotic species, Eurasian in origin, was first discovered in North America in Quebec, Canada, in 2008 (Landry et al. 2013) and reported in United States in 2016 (Harrison et al. 2016). *D. depressana* consumes flowers and immature fruits of *P. sativa* and *Daucus carota* (wild carrot) in North America (Harrison et al. 2016) and in its native range is associated with at least a dozen apiaceous genera in a diversity of tribes (Table 1). While *P. sativa* produces high amounts of furanocoumarins, particularly the linear furanocoumarin xanthotoxin (Zangerl and Berenbaum 2003), *D. carota* fruits contain linear but not angular furanocoumarins (Khalil et al. 2018), which do not exhibit the same phototoxic activity characteristic of linear furanocoumarins. Although *D. depressana* has been reported to feed on "cow parsnip" in Europe (Ovsyannikova and Grichanov 2021), it has not yet been reported to feed on any *Heracleum* species in North America. Taken together, these

components of the ecology of *D. depressana* suggest that its capacity for metabolizing furanocoumarins may be limited relative to *D. radiella*.

Thus, the recent appearance of *D. depressana* in central Illinois provided a unique opportunity to test the hypothesis that the detoxification capacity of a family-specialist herbivore is likely to be limited in comparison to the detoxification capacity of a super-specialist herbivore relative to the principal defensive chemicals across their range of hostplants. A multifaceted approach, with direct experimental tests of the metabolic activity and development of *D. depressana* interpreted in the context of the evolutionary history of *Depressaria* species and their hostplants, can shed light on the evolutionary history of association with plants containing furanocoumarins as well as provide a preliminary basis for evaluating the likelihood of this species to colonize native North American plant species, an important issue for evaluating potential adverse ecological impacts of invasive herbivores. To achieve these goals, we conducted midgut enzymatic assays to compare the efficiency with which furanocoumarins are metabolized by these two *Depressaria* species, assessed the ability of *D. depressana* to utilize hostplants varying in furanocoumarin content and composition, including a native species (*Zizia aurea*, golden alexanders), and reconstructed the phylogeny of *Depressaria* in the context of acquisition of furanocoumarin-containing hostplants.

Bucheli et al. (2010) presented the most comprehensive species-level *Depressaria* phylogeny to date. This phylogeny was constructed using a parsimony analysis on a dataset of 47 morphological characters. Hostplant and geographic associations were mapped onto the consensus tree. Hostplant family was used as a proxy for presence of furanocoumarins in hostplants. On the basis of coevolutionary theories proposed by Ehrlich and Raven (1964) and Berenbaum (1983), Bucheli et al. (2010) predicted that more derived species of *Depressaria*

would show increasingly specialized feeding on hostplant families possessing furanocoumarins but could find no evidence for that pattern in their analysis. Using COI barcodes with morphological data, as well as incorporating a more comprehensive review of hostplant associations, I revisited this phylogenetic analysis with special consideration of the phylogenetic placement of *D. depressana*.

METHODS

Three experiments were performed to evaluate the ecological capacity of two species of *Depressaria* to detoxify furanocoumarins and utilize species containing these chemicals as hosts within the context of the evolutionary history of the acquisition of furanocoumarin-containing hostplants within the genus. In Experiment 1, we compared the rate of midgut enzymatic metabolism of two furanocoumarins, representing linear and angular configurations, between *D. depressana* and *D. radiella* sampled from two populations differing in hostplant availability. In Experiment 2, we examined hostplant suitability by calculating gravimetric estimates of performance of *D. depressana* consuming tissues of actual or potential hostplants in comparison with those consuming a semi-defined artificial diet. In Experiment 3, we performed a phylogenetic analysis to infer changes in ancestral hostplant associations throughout the evolutionary history of the genus *Depressaria*.

Experimental Animals

Depressaria radiella were collected as eggs from the underside of hostplant leaves and reared to ultimate instar under laboratory conditions prior to experimentation. Eggs from a source population with *P. sativa* as the sole available hostplant were collected at Phillips Tract

(40.12966, -88.14390), an oldfield maintained by University of Illinois Urbana-Champaign (UIUC) in central Champaign County. Populations of *D. radiella* have been observed at this location at least since 1974 (Thompson and Price 1977). Eggs from a source population with *H. maximum* as the sole available hostplant were collected at Hart Woods (40.22880, -88.35639), a densely forested woodlot in northwest Champaign County also managed by UIUC. Populations of *D. radiella* have been recorded at this location since 1984 (Berenbaum and Zangerl 1991).

Populations of *D. depressana* were first recorded at Phillips Tract in 2015, with larvae observed feeding on umbels of *P. sativa* and *Daucus carota* (Harrison et al. 2016). In 2019, another population of *D. depressana* was discovered infesting umbels of *D. carota* in a roadside lot in southeast Urbana in 2019 (*personal observation*) (40.08227, -88.19002). Multiple instars of *Depressaria depressana* were collected from the umbels of either *P. sativa* at Phillips Tract or *D. carota* at the southeast Urbana site and reared through to adulthood and allowed to mate and lay eggs in the laboratory. Ultimate instar *D. depressana* larvae of the subsequent generation were used for assays.

For both species, larvae were housed in 1 oz. (28 mL) Solo® cups lined with 5 g of semi-defined artificial diet (hereafter, artificial diet) (Nitao and Berenbaum 1988) and were allowed to feed *ad libitum*. Laboratory colonies were maintained at 27 $\pm$ 4ºC and exposed to a 16:8 L:D photoperiod. All wild parsnip, cow parsnip, and wild carrot fruit samples were collected from field sites from which larvae were collected. Fruits of *Zizia aurea* were collected from a wildflower garden across from Morrill Hall on the UIUC campus (40.1087, -88.2244).

Chemicals

The furanocoumarins used in this experiment had the purities ≥ 98% –xanthotoxin was purchased from Sigma-Aldrich (St. Louis, MO), sphondin was purchased from INDOFINE Chemical (Hillsborough, NJ), and bergapten was purchased from TCI America (Portland, OR). Ingredients for the semi-defined artificial diet used to rear *D. radiella* and *D. depressana* were purchased from Sigma-Aldrich (St. Louis, MO), with the exception of wheat germ (Continental Mills, Seattle, WA) and wheat germ oil (Viobin, Monticello, IL), which were purchased locally. All chemicals used for the midgut bioassay were obtained from Sigma-Aldrich (St. Louis, MO). HPLC-grade and higher-grade solvents, including cyclohexane and 1-butanol, from Alfa Aesar (Ward Hill, MA), and diethylether from Fisher Chemical (Pittsburgh, PA) were used to make the mobile phase for analysis by high-pressure liquid chromatography.

Experiment 1: Comparative Furanocoumarin Metabolism Assays

Depressaria depressana and individuals from both populations of *D. radiella* were sampled three days after their ultimate larval molt. Tissues were processed following the protocol outlined by Berenbaum and Zangerl (2006). Midguts were dissected on ice in a dissection buffer containing phenylmethylsulfonylfluoride added to Crankshaw's solution (Crankshaw et al. 1979). They were then homogenized in a glass tube with a glass pestle in 100 µL grinding buffer, containing dissection buffer and additional leupeptin. Homogenates were then added to a 1.5 mL microcentrifuge tube along with glycerol and stored at -80ºC for later analysis.

Once the homogenates of all populations were collected, they were thawed on ice and transferred to a 15 mL Falcon conical centrifuge tube (Thermo Fischer Scientific, Waltham, MA)

containing 300 µL reaction mixture of 0.1 M, pH 7.8, phosphate buffer, with an NADPH-regenerating system and the substrate, either 10 mM xanthotoxin or 10 mM sphondin, was added. Tubes were then transferred to a 30ºC water bath for 25 min, after which time 400 µL of ice-cold ethyl acetate, containing 10 mM bergapten as the internal standard, was used to stop the reactions and to extract the furanocoumarins. The tubes were then vortexed immediately and centrifuged and 200 µL of the supernatant in the top layer of ethyl acetate were removed for analysis by high-pressure liquid chromatography (HPLC) to quantify unmetabolized furanocoumarins. A 4.6 x 250 mm Waters Analytical column (Part #PSS830115. Waters, Milford, MA) was used in conjunction with a Waters Millipore 712 WISP (Waters, Milford, MA), a Waters 501 HPLC Pump (Waters, Milford, MA), and a Waters 490E Programmable Multiwavelength Detector (Waters, Milford, MA). The furanocoumarins were eluted at a flow rate of 1.5 mL/min with a mobile phase consisted of 80% cyclohexane, 18% diethyl ether, and 2% 1-butanol, and detection was at 254 nm. Chromatogram peak integration analysis was performed using software developed in-house through LabVIEW (National Instruments, Austin, TX). Assumptions of normality and variance homogeneity were tested via Shapiro-Wilk test and Bartlett respectively. A one-way analysis of variance (ANOVA) paired with post-hoc Tukey's HSD test was performed in RStudio version 1.1.419 (Boston, MA) to test for significant difference among diet treatments.

Experiment 2: Gravimetric Feeding Efficiency Assays

Depressaria depressana larvae were reared to ultimate instar, whereupon 80 individuals were collected and deprived of food for 24 h to ensure the complete evacuation of gut contents before obtaining the fresh weight. Twenty individuals per treatment were transferred into

separate 28 mL (1 oz.) Solo© cups containing experimental diet. The five experimental diets for this analysis included approximately 3.0 g of artificial diet, 3.0 g of 0.3% xanthotoxin in artificial diet, 1.5 g *D. carota* immature seeds, 1.5 g *P. sativa* immature seeds, and 1.5 g *Z. aurea* immature seeds. A concentration of 0.3% xanthotoxin was used because this level represents the average xanthotoxin content in *P. sativa* seeds in central Illinois (Berenbaum and Zangerl 2006). *Zizia aurea* was selected as a treatment because this species is an umbellifer native to North America with low furanocoumarin production (Berenbaum 1981) and therefore represents a potential novel hostplant for *D. depressana*. After a 24 h feeding period, the larvae, frass, and remaining diet were separated into labeled 1 oz. (28 mL) cups and relocated to a drying oven set to 60ºC for 5 days. The contents of each cup were weighed after the drying period to obtain the post-experiment dry weights. Pre-experiment dry weights, representing the initial dry weight, were calculated using a separate group of 10 larvae for each diet and calculated by dividing fresh weight by dry weight and averaging the measurements within each treatment. Four measures of efficiency were calculated as outlined by Waldbauer et al. (1968): Efficiency of conversion of ingested food (ECI), efficiency of conversion of digested food (ECD), relative growth rate (RGR), and relative consumption rate (RCR).[1] Data analysis was performed in SPSS version 27 (IBM, Armonk, NY). In each test, the response variable was square-root transformed to meet assumptions of normality, which were tested on residuals via Shapiro-Wilk normality test. This was necessary as initial larval weight and absolute consumption varied across samples used in this experiment. A Bartlett test was implemented to test assumptions of equal variance. One-way

[1] ECI = biomass gain/diet ingested. Biomass gain represents the converted dry weight of the larva at 0 h minus the dry weight of the larva at 24 h. Diet ingested represents the diet dry weights at 0 h minus diet dry weights at 24 h. ECD = biomass gain/(consumption – frass). Consumption represents converted dry weights of the diet at 0 h minus the dry weights of the food at 24 h. RGR = biomass gain/larval mass. RCR = consumption/larval mass. Larval mass represents the converted dry weights of the larvae at 0 h.

ANOVA and ANCOVA analyses were performed to test for the significances of differences ($\alpha = 0.05$).

Experiment 3: *Depressaria* Phylogeny and Hostplant Ancestral State Reconstruction

Barcode analysis was incorporated into the morphology-based phylogeny of Bucheli et al. (2010). The COI analysis incorporated 60 total samples, including 53 *Depressaria* individuals representing 41 total species within the ingroup, and 7 *Agonopterix* individuals, representing 5 total species, as outgroups. These taxa were selected based on the availability of COI barcodes on the BOLD database (Ratnasingham and Hebert 2007) and availability of reliable hostplant records (Table 1). Reliability of hostplant record information was assessed with reference to reports in the published literature. Mitochondrial COI was incorporated into this analysis as it is particularly useful at providing resolution for more derived clades of *Depressaria,* an issue encountered by Bucheli et al. (2010). COI barcodes were aligned in Geneious (2021.1.1) using the MAFFT version 7.450 alignment algorithm (Katoh and Standley 2008) with default parameters. The COI dataset was then partitioned by codon position to account for variable mutation rates at each position. A dataset of 33 morphological characters was obtained from Bucheli et al. (2010) (Table 2) and incorporated into the phylogenetic reconstruction. Fourteen morphological characters from the original dataset of 47 available traits (Bucheli et al. 2010) were not used in this analysis as they were not taxonomically informative within our sample set of 60 taxa.

Maximum likelihood (ML) analysis was performed with RAxML version 8.2.12 (Stamakis 2014). PartitionFinder (Lanfear et al. 2012) was used to select GTRGAMMA as the best fitting nucleotide substitution model under AIC and the Markov k (Mk) model for

morphological character evolution. A general parametric constraint was implemented to establish *Agonopterix* and *Depressaria* as monophyletic. Support values were obtained via 1000 bootstrap replicates.

Bayesian phylogenetic (BP) analysis was performed using BEAST version 2.6.0 (Bouckaert et al. 2019). Site model averaging was implemented using the bModelTest package (Bouckaert and Drummond 2017) for each codon position and morphological characters. A relaxed clock log normal model was applied with a 0.0115 clock rate for COI nucleotide mutation rate (Brower 1994) with rates for morphological characters left as estimated with no specified clock. As in the maximum likelihood analysis, monophyletic constraint priors were applied to *Agonopterix* and *Depressaria*. The BP analysis ran for 150 million Markov chain Monte Carlo (MCMC) generations beginning from a random tree with every chain sampling every 5,000th cycle. Tracer version 1.7.2 (Rambaut et al. 2018) was used to ensure effective sample size (ESS) values for all parameters were greater than 200. A maximum clade credibility tree was generated in TreeAnnotator (Bouckaert et al. 2019) with median node heights and 10% burn-in.

The BP tree was loaded into RASP (Yu et al. 2020) for a multistate reconstruction of ancestral hostplant associations. Hostplant families were coded as traits in RASP as either Asteraceae (A), Apiaceae (B), Fabaceae (C), Caprifoliaceae (D), Rutaceae (E), Betulaceae (F), Salicaeae (G), or a combination of these for species that feed upon multiple hostplant families. Trait evolution was evaluated using Bayesian Binary MCMC. The resulting tree was edited in Adobe Illustrator version 25.4.1 (Adobe Inc. 2021) where maximum likelihood bootstrap support values were added.

RESULTS

Experiment 1: Gravimetric Feeding Efficiency Assays

Diet type differentially affected absolute weight gain in *D. depressana* larvae, with *D. carota* resulting in a greater increase in larval mass relative to all other diet types (*ANOVA*, Tukey's HSD, $P < 0.05$) (Fig. 1.2a). Diet type also affected absolute consumption, with the three fruit tissue diets resulting in significantly lower overall consumption relative to the 0.3% xanthotoxin artificial diet and unsupplemented artificial diet being intermediate in terms of consumption (*ANOVA*, Tukey's HSD, $P < 0.05$). The ANCOVA analysis for ECI revealed that both diet ($F = 6.672$, $df = 4, 94$, $P < 0.05$) and rate of food ingestion ($F = 11.880$, $df = 4, 94$, $P < 0.05$) affected larval mass. Similarly, the ECD ANCOVA analysis determined larval mass increase was significantly affected by diet ($F = 10.513$, $df = 4, 94$, $P < 0.05$) and amount of digested food ($F = 6.604$, $df = 4, 94$, $P < 0.05$). ANCOVA analysis for relative growth rate (RGR) revealed that diet affected larval weight gain ($F = 4.291$, $df = 4, 94$, $P < 0.05$), but that initial weight did not ($F < 0.01$, $df = 4, 94$, $P = 0.996$). Lastly, ANCOVA analysis for relative consumption rate (RCR) found that diet affected rates of larval consumption ($F = 4.261$, $df = 4, 94$, $P < 0.05$), but that initial weight did not ($F = 0.244$, $df = 4, 94$, $P = 0.622$).

Experiment 2: Comparative Furanocoumarin Metabolism Assays

Furanocoumarin metabolism is reported as mean percentage decrease of the substrate, either xanthotoxin or sphondin, in the midgut extracts of the same individuals between 0 mins and 25 mins of the bioassay. Metabolism of xanthotoxin (Fig. 1.3a) did not differ between individuals from populations of *D. radiella* associated exclusively with either *P. sativa* and *H. maximum*, with a mean decrease of 39.3% and 38.9% in initial xanthotoxin content, respectively

(*ANOVA*, Tukey HSD, $P < 0.05$). *D. radiella* larvae from both populations, however, exhibited significantly higher xanthotoxin metabolism than *D. depressana* (*ANOVA*, Tukey HSD, $P < 0.05$), which metabolized only 19.6% of the initial xanthotoxin content (Fig. 1.3b). *D. radiella* from *H. maximum* populations metabolized 39.0% of the initial sphondin substrate, which was significantly greater than did larvae from *P. sativa* populations, which metabolized 27.9% (*ANOVA*, Tukey HSD, $P < 0.05$). As with xanthotoxin, both populations of *D. radiella* metabolized sphondin more efficiently than *D. depressana* larvae, which metabolized 11.3% of the initial substrate (*ANOVA*, Tukey HSD, $P < 0.05$).

Experiment 3: *Depressaria* Phylogeny and Hostplant Ancestral State Reconstruction

The COI dataset comprised 658 aligned base pairs. The combined maximum likelihood (ML) and Bayesian phylogenetic (BP) analyses on the COI barcode and morphology dataset are shown in Fig. 1.4, with corresponding posterior probabilities and bootstrap support values. There were 58 internal nodes, of which 33 display posterior probabilities of 0.9 or higher and 23 with bootstrap support values about 70%. In general, nodes with high support values across both measures of support tended to be more derived, except when separating individuals of the same species. Of the 58 nodes, ~19% displayed incongruence between the ML and BP analyses. Each tree is given separately in Fig. 1.3.

The ancestral hostplants of *Depressaria* and *Agonopterix* were estimated for all 58 nodes (Fig. 1.4). The probability of feeding on Apiaceae as compared to other hostplant families was 90.62% for the *Depressaria* and *Agonopterix* most recent common ancestor (MRCA). The most recent common ancestor to the *Agonopterix* clade was predicted to use as hostplants species within the Apiaceae with a 77.11% probability, whereas the most recent common ancestor to the

Depressaria had a 74.73% probability of utilizing apiaceous plants as hosts. *Depressaria radiella* belongs to the clade containing *D. libanotidella*, *D. pimpinellae*, and *D. velox*, and its most recent common ancestor had a 95.68% probability of feeding upon apiaceous hosts. The most recent common ancestor of the clade containing *D. depressana* and *D. chaerophylli* was predicted to utilize Apiaceae with a 99.70% probability.

DISCUSSION

Dietary xanthotoxin causes a decrease in the efficiency with which *D. depressana* can convert ingested and digested food to biomass (Figure 1.2). Ultimately, the presence of xanthotoxin, both in *P. sativa* and in artificial diet, results in reduced growth rate. Carroll (2003) observed a similar reduction in growth rate in *D. radiella* in response to dietary xanthotoxin and found that these effects can be ameliorated by presence of lutein, a carotenoid possessing antioxidant properties. Previous studies report that *D. radiella* larvae do not discriminate against diet containing xanthotoxin when presented with an alternative diet lacking xanthotoxin (Berenbaum and Zangerl 1992) and even increase their rate of consumption (Berenbaum et al. 1989), unlike other Lepidoptera for which xanthotoxin acts as a feeding deterrent (Berenbaum 1995). Additionally, *a priori* exposure to furanocoumarins in the source population influenced the capacity of *D. radiella* to metabolize furanocoumarins (Berenbaum and Zangerl 1998). *D. depressana* larvae in this analysis were sourced from a population feeding exclusively on *D. carota*, lacking nearby *P. sativa* that could potentially exert selective pressure for xanthotoxin detoxification as alternative hosts. The increase in efficiency of conversion of ingested and digested *D. carota*, and subsequent increased growth rate, even relative to the artificial diet not supplemented with xanthotoxin, suggests the presence of beneficial dietary components that

promote development. While *D. depressana* displayed significantly reduced performance on *Z. aurea* fruits relative to performance on *D. carota* fruits, conversion efficiencies and growth rate were not reduced relative to *P. sativa*, suggesting that *D. depressana* could potentially establish populations on *Z. aurea* as an alternate host in areas of invasion, with potential consequences for the survival of vulnerable or imperiled *Z. aurea* populations.

That larvae from both populations of *D. radiella* displayed markedly higher xanthotoxin and sphondin metabolism than did *D. depressana* larvae is consistent with the expectation that family-specialists display lower levels of resistance to relatively rare defense chemicals compared to family-superspecialists. With respect to *D. radiella*, differences in furanocoumarin metabolism across geographically separated populations feeding on *P. sativa* varying in chemical profiles have been well documented (Zangerl and Berenbaum 2003; Berenbaum and Zangerl 2006). Proximity to *H. maximum* alters the intensity of selection and therefore precision of the phenotype match between the detoxification profile of *D. radiella* larvae and the furanocoumarin defense profile of associated *P. sativa* populations (Zangerl and Berenbaum 2003). Immature seeds of *H. maximum* can contain up to 11 times the total amount of furancoumarins than do immature seeds of *P. sativa*; as well, the furanocoumarins of cow parsnip contain angular furanocoumarins in higher proportions (Berenbaum and Zangerl 1991). As such, *D. radiella* collected from *H. maximum* appear to have responded to selective pressure to adapt to higher concentrations of sphondin, as evidenced by the HPLC results, providing preliminary evidence for local host-races of *D. radiella*.

Phylogenetic position of several taxa differed between our analysis and that of Bucheli et al. (2010). Most notable is the placement of *D. dictamnella.* This Old World species, mostly concentrated in Portugal and Spain, has as its primary host *Dictamnus albus* (Krone 1911), a

rutaceous species that produces the linear furanocoumarins xanthotoxin and bergapten, as well as trace amounts of psoralen (Zobel and Brown 1990). This pattern suggests that adaptation to furanocoumarins is a basal trait in the evolution of *Depressaria* or perhaps even earlier in ancestral lineages predating the *Depressaria* and *Agonopterix* split. The phylogenetic position of *D. depressana* also differs greatly between our analysis and the analysis of Bucheli et al. (2010). Bucheli et al. (2010) placed *D. depressana* as sister to the remaining unresolved clade termed the *artemisiae* group (*D. chaerophylli*, *D. atrostrigella*, *D. artemisiae*, *D. absynthiella*, and *D. heydenii*), which is characterized as containing Old World species with a bisetose SV seta condition on the A1 segment; by contrast, our analysis positions *D. depressana* as sister to *D. chaerophylli*, though support is relatively low (pb = 0.8, bs = 38) (Fig. 1.4). The remaining species of the *artemisiae* group, save for *D. atrostrigella* (omitted from our study), are repositioned within a more derived clade sister to *D. veneficella*, *D. discipunctella*, and *D. silesiaca*, whose hostplants include members of the Asteraceae and Apiaceae. Further, our analysis shows that this new clade is more closely related to the group Bucheli et al. (2010) termed the *pastinacella* group (*D. badiella*, *D. bupleurella*, *D. libanotidella*, *D. pimpinellae*, *D. velox*, and *D. radiella*), which are Old World species that feed on a combination of Apiaceae and Asteraceae and also possess bisetose SV setae. With reasonably high support, our analysis further resolves the relationships within the clade containing *D. radiella* with the group containing *D. badiella* and *D. bupleurella* as sister to the remaining taxa and therein *D. radiella* as sister to *D. libanotidella*, *D. pimpinellae*, and *D. velox*. Additional differences between phylogenies include the dissolution of the *discipunctella* group, and the placement of the *betina* group as sister to *D. albipunctella* within the *douglasella* group. The clade containing the *betina* and *douglasella* groups comprise both New and Old World species that utilize as hostplants

species in the Apiaceae and Asteraceae. Despite the many limitations of this study—use of only mitochondrial COI in a molecular dataset to supplement the morphological data, incomplete hostplant records, and differential coverage of furanocoumarin distributions in the literature, our analysis generally shows strong support for intra-genus relationships.

As for testing the escape-and-radiate hypothesis, definitive conclusions are more difficult to draw. Bucheli et al. (2010) evaluated *Depressaria* as a test of the escape-and-radiate hypothesis across several different axes: furanocoumarin specialization, plant tissue specialization (flowers versus leaves), and habitat specialization (woody versus herbaceous). They reached the conclusion that association with furanocoumarin-producing hostplants (with plant family serving as a proxy) is a weak predictor of species-level evolution within *Depressaria*, as this trait predates the genus with feeding on plants in the Asteraceae (assumed to lack furanocoumarins) being the result of multiple independent instances of convergent evolution. However, because broad-scale heterogeneity of furanocoumarin production exists within plant families, even the Apiaceae, and that plant species that produce furanocoumarins do so in varying amounts, proportions, and chemical complexity, plant family is not a precise proxy for plant chemistry (furanocoumarins are not reported to occur in some apiaceous tribes and Kinghorn et al. (2017) report finding furanocoumarins in at least two asteraceous genera). Bauri et al. (2016) reported finding a photobiologically active furanocoumarin from *Artemisia reticulata*, a species in an asteraceous genus that is a hostplant for multiple *Depressaria* species. A further analysis of hostplant chemical profiles is warranted. Natural product discovery is proceeding apace; according to Sarker et al. (2017), "Well over 400 coumarin isolations were reported in the years 2014 and 2015," so absence of records of furanocoumarins in any particular plant species may well represent absence of investigative effort rather than biological reality.

Another obstacle to drawing any definitive conclusion about testing the escape-and-radiate hypothesis is, as mentioned, the incomplete nature of host records for many species in this group. (1964). Within the clade contain *D. radiella*, only one species, *D. pimpinellae*, utilizes a host plant species known to produce angular furanocoumarins (Fig. 1.4), *Pimpinella* spp. However, *D. pimpinellae* is most closely related to *D. velox*, and that group is sister to *D. libanotidella*; although neither of these species are reported to utilize plants that produce angular furanocoumarins (Table 1), hostplant records are rare and almost certainly incomplete. Angular furanocoumarin detoxification appears to be a trait independently evolved in several lineages in both *Depressaria* and *Agonopterix*, as is the case with *A. angelicella* (Table 1). This contrasts with apparent evolutionary trends among species within the genus *Papilio* (Lepidoptera: Papilionidae), which are a better fit for the escape-and-radiate model with respect to angular furanocoumarin detoxification (Sperling and Feeny 1995). Sperling and Feeny (1995) found that evolution of angular furanocoumarin tolerance likely led to the diversification of the *P. machaon* group as this trait would have led to wider hostplant availability.

Many studies examining plant-insect interactions were founded on the premise that specialist herbivores are better adapted to overcome the defensive chemistry of their hostplants and will thus outperform generalists (Scriber and Feeny 1979). However, recent studies call this long-maintained assumption into question because they often fail to take into consideration confounding ecological factors such as feeding guild, plant response, behavioral idiosyncrasies, and the effect of trophic-level interactions (Ali and Agrawal 2012; Smilanich et al 2016; Loxdale and Harvey 2016). Additionally, the terms ‘generalist’ and ‘specialist’ may also oversimplify a continuous spectrum of insect diet breadth (Loxdale and Harvey 2016). Rothwell and Holeski (2020) conducted a meta-analysis incorporating 45 studies and found evidence that specialist

insects do outperform generalists in terms of growth, but not fecundity or survival. However, the need remains for further consideration of insects occupying the middle portion of the diet breadth spectrum.

Diet breadth even within a hostplant family may provide insights into the likelihood of success of a specialist group in invading new habitats and colonizing novel hostplants. Collectively, our work suggests that *D. depressana* may not be well suited to adopt *H. maximum* as a novel host. This insect is not reported to utilize plant species producing high levels of angular furanocoumarins as hosts in its native range and, according to our analysis, belongs to a clade containing species that do not regularly ingest and metabolize angular furanocoumarins in their diet. Moreover, because of its expanded host range, the availability of less toxic alternate hostplants may result in relaxed selective pressure to colonize *H. maximum*. While *D. depressana* metabolizes sphondin to a certain degree, it does so relatively inefficiently compared to *D. radiella*. Because *D. depressana* can feed and grow on *P. sativa* despite metabolizing xanthotoxin at a rate much lower than that of *D. radiella*, however, direct tests of larval development on *H. maximum* under controlled laboratory conditions could be clarifying. Native apiaceous plants that produce low levels of linear furanocoumarins are much more likely to be colonized by *D. depressana*, as evidenced by our feeding efficiency assays. While growth rate and efficiency of conversion of ingestion and digestion of *Z. aurea* to larval biomass were reduced compared to *D. carota*, they did not significantly differ from *P. sativa* or semi-defined artificial diet, suggesting that larvae may be able to utilize *Z. aurea* as an alternate host as it continues to expand west across North America.

Increasing globalization of trade essentially guarantees that, in the future, species of Apiaceae specialists in the Depressariidae will be among those with distributions that expand to

new countries and new continents. In view of both the economic importance of apiaceous plants as sources of herbs, spices, and vegetables and the conservation concerns about many endemic species in the family, efforts to understand the nature of the evolutionary association between these plants and their specialist enemies may become increasingly valuable. Particularly pertinent in this regard is the impact that invasive depressariines have upon native, vulnerable umbellifers. For example, three species of *Lomatium* (*L. greenmanii*, *L. erythrocarpum*, and *L. oreganum*), high alpine specialists endemic to states in the Pacific Northwest in N. America, are currently under consideration for increased conservation efforts and may be highly susceptible to the added selective impact of invasive depressariines (Ottenlips et al. 2020). Increased attention paid to the chemical ecology of invasive species could further bolster the predictive power of models attempting to evaluate the damage of invasive *Depressaria.*

TABLES AND FIGURES

Table 1.1 Hostplant records for all taxa in the phylogenetic analysis. Current distribution of all *Depressaria* and *Agonopterix* is identified to geographic region and hostplants are identified to family and genus or species depending on availability of information in the literature.

Species	***Region***	***Hostplant Family***	***Hostplants***	***Hostplant Records***
Agonopterix angelicella	Palearctic	Apiaceae	*Angelica*	Palm (1989)
		"	*Laserpitium*	"
		"	*Aegopodium*	"
		"	*Pimpinella saxifraga*	"
		"	*Pastinaca*	"
		"	*Heracleum*	"
Agonopterix canadensis	Nearctic	Asteraceae	*Senecio serra*	Hodges (1983)
Agonopterix clemensella	Nearctic	Apiaceae	*Pastinaca sativa*	Hodges (1983)
Agonopterix gelidella	Nearctic	Betulaceae, Salicaceae	*Salix*	Hodges (1983)
Agonopterix heracliana	Palearctic	Apiaceae	*Heracleum*	Palm (1989)
		"	*Chaerophyllum*	"
		"	*Torilis*	"
		"	*Angelica silvestris*	"
		"	*Aegopodium*	"
		"	*Daucus*	"
		"	*Seseli*	"
		"	*Carum*	"
		"	*Peucedanum*	"
		"	*Conium*	"
		"	*Oenanthe*	"
		"	*Silaum*	"
Agonopterix nebulosa	Nearctic	Asteraceae	*Antennaria plantaginifolia*	Hodges (1983)
Agonopterix robiniella	Nearctic	Apiaceae	*Sanicula*	Hodges (1983)
		Fabaceae	*Robinia pseudoacacia*	"
Depressaria absynthiella	Palearctic	Asteraceae	*Artemisia absinthium*	Herrich-Schaffer (1856)
		"	*Artemisia thuscula*	"
Depressaria albipunctella	Palearctic	Apiaceae	*Daucus*	Palm (1989)
		"	*Conium*	"
		"	*Torilis*	"
		"	*Anthrispicus*	"
		"	*Chaerophyllum*	"
		"	*Pimpinella*	"
		"	*Seseli*	"
Depressaria alienella	Nearctic	Asteraceae	*Achillea*	Walsingham (1881)
		"	*Artemisia*	Clarke (1941)
Depressaria angelicivora	Nearctic	Apiaceae	*Angelica arguta*	Clarke (1952)
Depressaria artemisiae	Palearctic	Asteraceae	*Artemisia campestris*	Palm (1989)
			Artemisia borealis	"
			Artemisia bottnica	

Table 1.1 (cont.)

Depressaria badiella	Palearctic	Apiaceae, Asteraceae	*Hypochoeris radiata* *Sonchus arvensis* *Taraxacum*	Palm (1989) " "
Depressaria beckmanni	Palearctic	Apiaceae	*Pimpinella major*	Wieser and Huemer (1997)
Depressaria betina	Nearctic	Apiaceae " " "	*Lomatium nudicaule* *Lomatium triternatum* *Lomatium columbianum* *Lomatium dissectum*	Hodges (1983) " " "
Depressaria bupleurella	Palearctic	Apiaceae	*Bupleurum falcatum*	Palm (1989)
Depressaria chaerophylli	Palearctic	Apiaceae " " "	*Chaerophyllum temulentum* *Chaerophyllum bulbosom* *Aegopodium* *Anthriscus sylvestris*	Palm (1989) " " "
Depressaria cinderella	Palearctic	Apiaceae	*Conopodium*	Buchner and Sumpich (2018)
Depressaria cinereocostella	Nearctic	Apiaceae " " " "	*Oxypolis rigidior* *Sium suave* *Cicuta maculata* *Carum carvi* *Ligusticum scoticum*	Hodges (1983) " " " "
Depressaria constancei	Nearctic	Apiaceae	*Lomatium californicum*	Hodges (1983)
Depressaria daucella	Holarctic	Apiaceae " " " " " " " " " "	*Cicuta* *Berula* *Carum* *Daucus* *Pastinaca* *Phellandrium* *Apium* *Laserpitium* *Oenanthe crocata* *Oenanthe sarmentosa* *Cicuta douglasii*	Palm (1989) " " " " " " " " Hodges (1983) "
Depressaria depressana	Holarctic	Apiaceae " " " "	*Daucus carota* *Pimpinella* *Pastinaca sativa* *Seseli* *Peucedanum* *Oreoselinum*	Palm (1989) " " " "
Depressaria dictamnella	Palearctic	Rutaceae	*Dictamnus albus*	Krone (1911)

Table 1.1 (cont.)

Depressaria discipunctella	Palearctic	Apiaceae	*Heracleum*	Palm (1989)
		"	*spondylium*	"
		"	*Pastinaca*	"
		"	*Angelica silvestris*	"
			Ferula	
Depressaria douglasella	Palearctic	Apiaceae	*Daucus*	Palm (1989)
		"	*Anthriscus*	"
		"	*Seseli*	"
		"	*Carum*	"
		"	*Pastinaca*	"
Depressaria eleanorae	Nearctic	Apiaceae	*Conioselinum chinense*	Clarke (1952)
Depressaria emeritella	Palearctic	Asteraceae	*Tanacetum vulgare*	Palm (1989)
Depressaria erinaceella	Palearctic	Asteraceae	*Cynara cardunculus*	Iglesias et al. (2002)
Depressaria heydenii	Palearctic	Apiaceae	*Heracleum austriacum*	Palm (1989)
Depressaria hofmanni	Palearctic	Apiaceae	*Seseli libanotis*	Requena et al. (2014)
		"	*Pastinaca sativa*	"
Depressaria lacticapitella	Palearctic	Apiaceae	*Athamanta cretensis*	Klimesch 1942
Depressaria leucocephala	Palearctic	Asteraceae	*Artemisia vulgaris*	Palm (1989)
Depressaria libanotidella	Palearctic	Apiaceae	*Seseli libanotis*	Palm (1989)
Depressaria marcella	Palearctic	Apiaceae	*Daucus carota*	Requena et al. (2014)
		"	*Foeniculum vulgare*	"
Depressaria moya	Nearctic	Apiaceae	*Lomatium vaginatum*	Hodges (1983)
Depressaria multifidae	Nearctic	Apiaceae	*Lomatium dissectum*	McKenna and Berenbaum (2003)
		"	*Lomatium grayi*	"
		"	*Pteryxia terebinthina*	"
Depressaria olerella	Palearctic	Asteraceae	*Achillea millefolium*	Palm (1989)
		"	*Tanacetum*	"
Depressaria pimpinellae	Palearctic	Apiaceae	*Pimpinella major*	Palm (1989)
		"	*Pimpinella saxifraga*	"
Depressaria pulcherrimella	Palearctic	Apiaceae	*Pimpinella saxifraga*	Palm (1989)
		"	*Conopodium*	"
		"	*Daucus*	"
		"	*Cnidium*	"
		"	*Bunium*	"
		Caprifoliaceae	*Valeriana*	"
		Asteraceae	*Centaurea*	"

Table 1.1 (cont.)

Depressaria radiella	Holarctic	Apiaceae " " " " "	*Pastinaca sativa* *Heracleum* *maximum* *Heracleum* *sphondylium* *Heracleum sibiricum* *Angelica* *Oenanthe silaifolia*	Palm (1989) Berenbaum and Zangerl (1991) Palm (1989) " " "
Depressaria silesiaca	Palearctic	Asteraceae "	*Achillea millefolium* *Artemisia vulgaris*	Palm (1989) "
Depressaria sordidatella	Palearctic	Apiaceae " " " " " "	*Anthriscus sylvestris* *Chaerophyllum* *temulum* *Pastinaca sativa* *Peucedanum* *Conium* *Angelica* *Heracleum*	Requena et al. (2014) " " " " " "
Depressaria tenebricosa	Palearctic	Apiaceae	*Conopodium majus*	
Depressaria togata	Nearctic	Apiaceae " " "	*Lomatium* *ambiguum* *Lomatium* *triternatum* *Perideridia* *bolanderi* *Pteryxia* *terebinthina*	Hodges (1983) " " "
Depressaria ultimella	Palearctic	Apiaceae " " " "	*Sium* *Oenanthe* *Berula* *Phellandrium* *Apium nodiflorum*	Palm (1989) " " " "
Depressaria ululana	Palearctic	Apiaceae	*Bunium* *bulbocastanum*	Requena et al. (2014)
Depressaria velox	Palearctic	Apiaceae "	*Ferula communis* *Seseli tortuosum*	Requena et al. (2014) "
Depressaria veneficella	Palearctic	Apiaceae	*Thapsia*	Requena et al. (2014)
Depressaria yakimae	Nearctic	Apiaceae	*Pteryxia* *terebinthina*	Clarke (1952)

Table 1.2 Morphological characters from Bucheli et al. (2010) used in this analysis.

CHARACTER	STATE
3. ANELLUS	0. without lateral lobes or projections 1. with lateral lobes
4. MESOTHORACIC LEG WITH SCALE TUFTS	0. absent 1. present at halfway and at apex
7. FOREWING WITH CU1 AND CU2	0. separate 1. stalked
9. HINDWING WITH M3 AND CU1	0. separate 1. stalked or connate
10. HINDWING WITH M3 AND CU1	0. connate with Cu2 1. removed from Cu2
12. UNCUS	0. absent 1. reduced 2. present
19. AEDEAGUS	0. tapering to a point 1. blunt
20. AEDEAGUS	0. straight or nearly so 1. moderate to strongle c-shaped
21. AEDEAGUS FLANGE	0. absent 1. single 2. double
22. VESICA OF AEDEAGUS	0. bare 1. with cornuti
23. CORNUTI	0. scale-like and numerous located in a patch 1. stout and inger-like and either single or a few in a row 2. saw tooth-like and numerous located at base of vesica
24. IF CORNUTI FINGER-LIKE	0. limited to middle of vesica 1. extending near tip of vesica
25. SACCULUS	0. without lobe or process basally 1. with a small indistinct distinct basal process 2. with a short or long basal process
26. BASAL PROCESS WITH SCALE-LIKE PROJECTIONS	0. absent 1. present only at tip 2. covering entire process
27. SCALE-LIKE PROJECTIONS OF BASAL PROCESS	0. fine 1. robust

Table 1.2 (cont.)

28. BASAL PROCESS OF SACCULUS	0. straight or nearly so or with inner margin slightly concave 1. highly curved with inner margin convex
30. VALVA WITH MEDIAL LOBE	0. absent 1. clearly distinct from sacculus 2. not clearly distinct from sacculus
31. DISTAL PROCESS	0. absent linear to curved and sometimes bifid at tips 2. quadrate
32. DISTAL PROCESS OF VALVE	0. free 1. not free
33. DISTALE PROCESS OF VALVE	0. straight 1. elbowed
34. APEX OF DISTAL PROCESS OF VALVE	0. rounded or pointed 1. bifid
35. COSTAL MARGIN OF VALVE	0. straight or nearly so 1. noticeably concave 2. noticeably convex
36. SHAPE OF VALVE	0. broadest at the base and tapering at 1/2 ti 1/3 length 1. broadest at base to nearly 5/6 in length or nearly straight 2. broadest at middle
37. CUCULLUS OF VALVE	0. rounded 1. pointed
38. COSTAL MARGIN OF VALVE	0. without process 1. with process located at least 3/4 middle of costa to tip of costa 2. located basally or at least 3/4 middle of costa
39. VALVE HAIRS	1. primarily located at cucullus 2. primarily located along costa, sacculus, and cucullus 3. centrally located
40. TRANSTILLA	0. absent 1. present
41. TRANSTILLA	0. membranous 1. sclerotized
42. LATERAL LOBES OF TRANSTILLA	0. absent 1. weakly developed 2. well developed

Table 1.2 (cont.)

43. VINCULUM	0. rounded 1. pointed
44. VINCULUM ANTERODORSAL PROCESS	0. not well developed 1. well developed
45. OSTIUM BURSAE	0. present anteriorly 1. near middle
46. DUCTUS BURSAE MEETS CORPUS BURSAE	0. at right angle 1. straight or slightly curved

Figure 1.1 *Depressaria depressana* feeding on native *Zizia aurea* (golden alexanders).

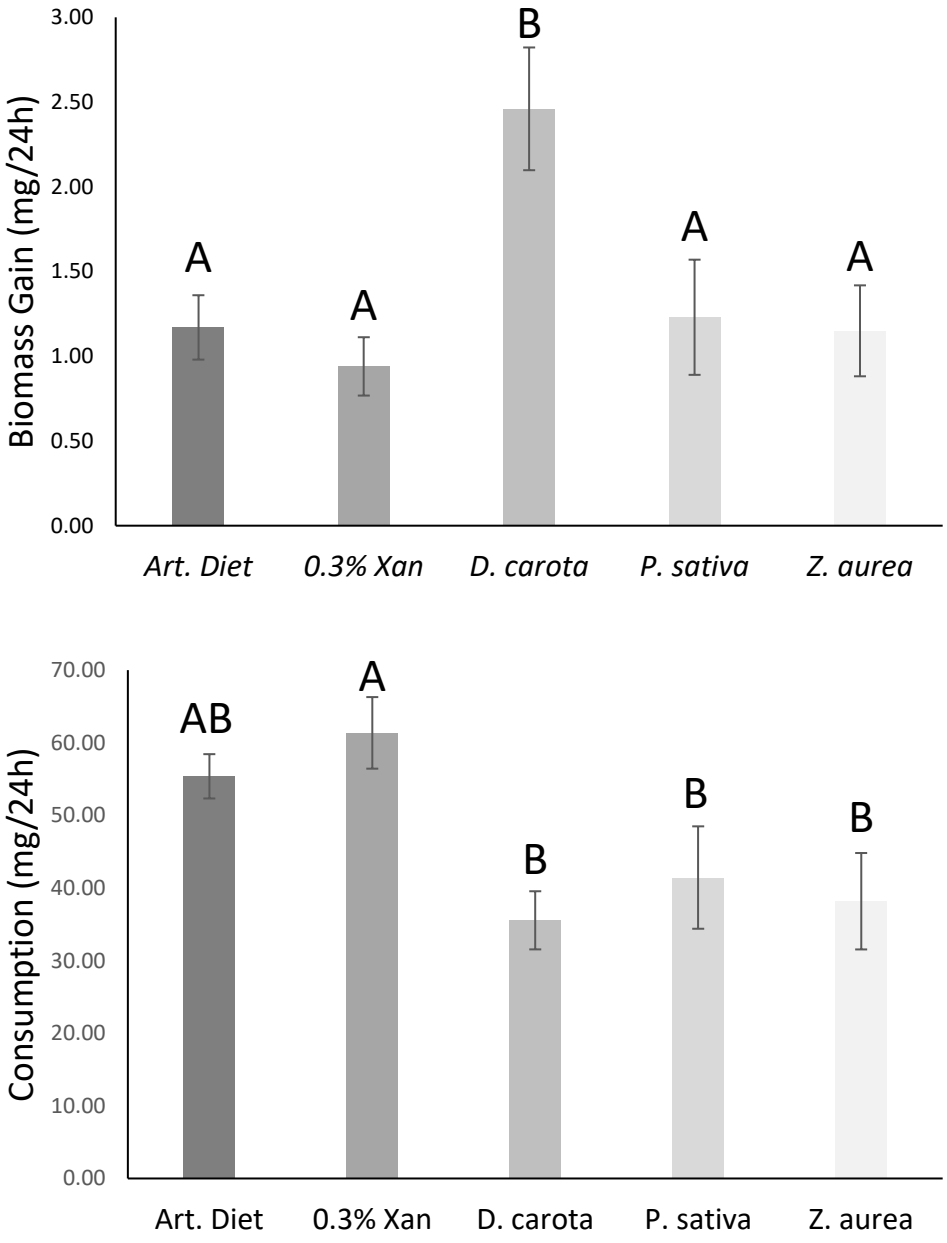

Figure 1.2 (a) Mean (± SE) rate of biomass gain, and **(b)** Mean (± SE) rate of consumption of *Depressaria depressana* after 24 hrs of feeding on either semi-defined artificial diet, 0.3% xanthotoxin in semi-defined artificial diet, *Daucus carota*, *Pastinaca sativa*, or *Zizia aurea*. Biomass gain was calculated by subtracting the converted dry weight (mg) of larvae at 0 h from larval dry weight (mg) at 24 hrs. Consumption was calculated by subtracting the converted dry weight (mg) of food at 0 h from the dry weight (mg) of food at 24 hrs. Columns marked with same uppercase letters denote no significant different (ANOVA, Tukey's HSD test, $P > 0.05$).

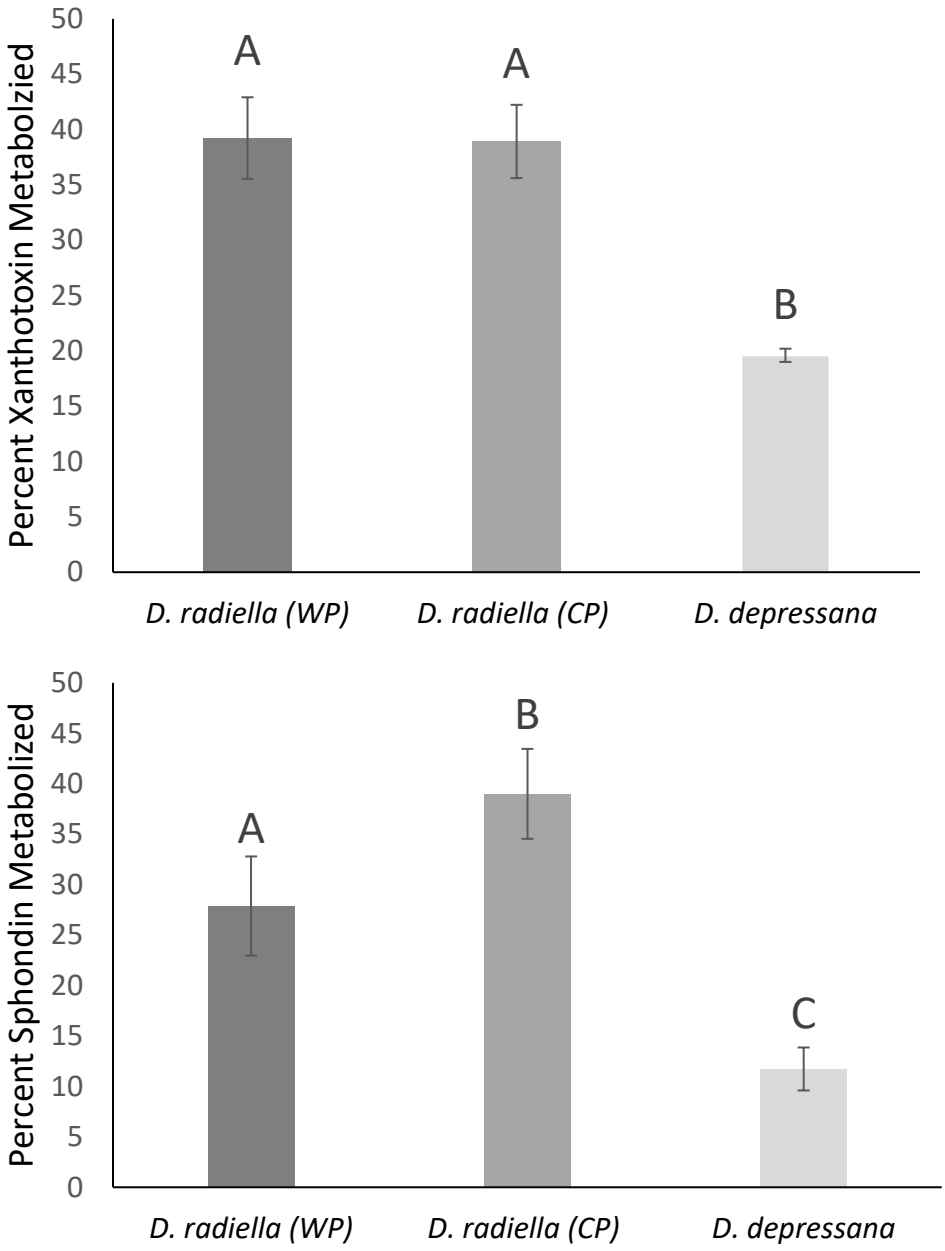

Figure 1.3 Mean (± SE) percentage decrease of (**a**) xanthotoxin and (**b**) sphondin among *Depressaria radiellia* collected from populations with wild parsnip (WP) as the sole hostplant, populations of *D. radiellia* with cow parsnip (CP) as the sole hostplant, and *Depressaria depressana* collected from wild parsnip. Columns marked with same uppercase letters denote no significant different (ANOVA, Tukey's HSD test, $P > 0.05$)."

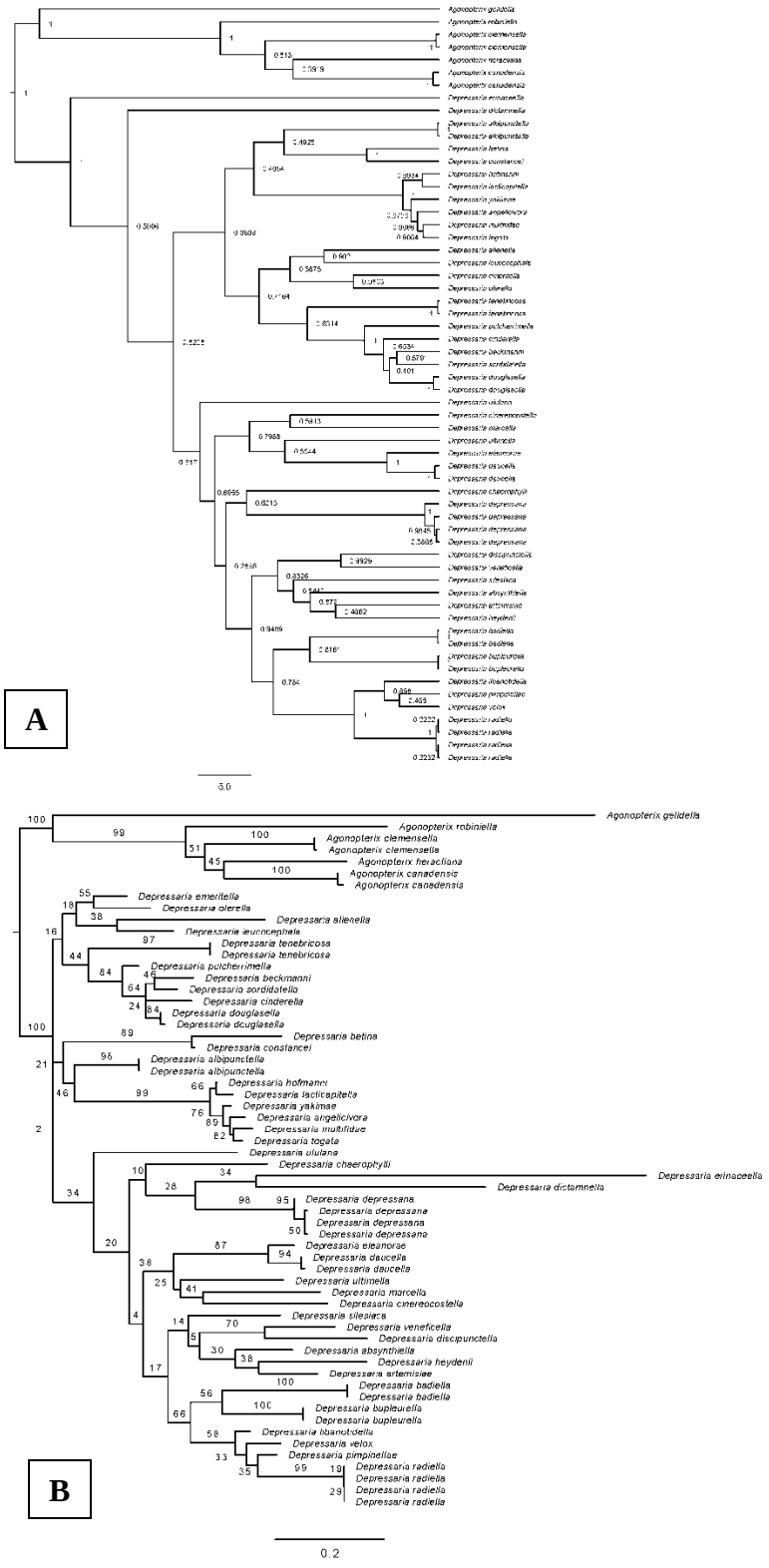

Figure 1.4 A) Bayesian phylogenetic (BP) analysis of COI. Numbers represent posterior probability support values for each node. B) Maximum likelihood (ML) analysis of COI. Numbers represent bootstrap support values for each node.

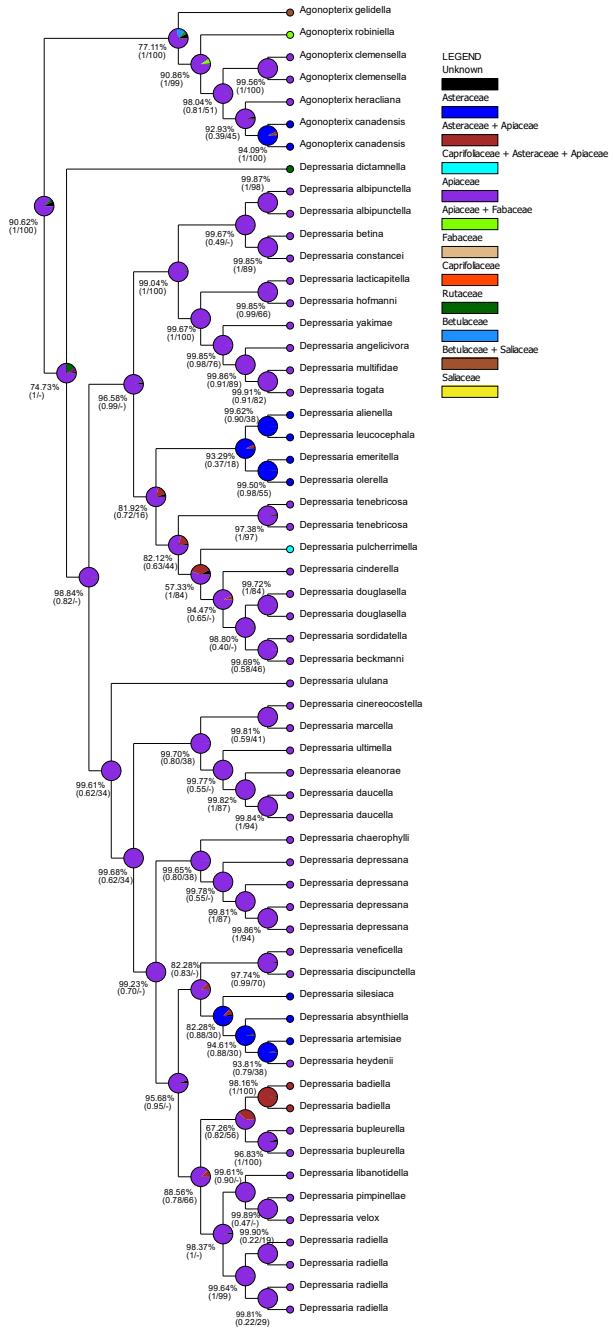

Figure 1.5 Cladogram resulting from Bayesian phylogenetic (BP) analysis the using COI barcode and morphology dataset retrieved from Bucheli et al. (2010) (Table 2). Pies at each node represent the probably of ancestral hostplant trait as determined from a Bayesian Binary MCMC multistate analysis. Traits were coded as (A) Asteraceae (B) Apiaceae (C) Asteraceae (C) Fabaceae (D) Caprifoliaceae (E) Rutaceae (F) Betulaceae (G) Salicaceae, or a combination of any of the above. Numbers indicate percent likelihood of the most probable ancestral hostplant state at each node, posterior probability from the BP analysis, and bootstrap support values from the maximum likelihood (ML) analysis. Incongruent topologies between BP and ML trees are indicated with a hyphen (-) in place of bootstap value.

REFERENCES

Ali JG, Agrawal, AA (2012) Specialist versus generalist herbivores and plant defense. Trends Plant Sci 17:293-302.

Bauri AK, Foro S, Nguyen Do NQ (2016) Crystal structure of a photobiologically active furanocoumarin from *Artemisia reticulata*. Acta Crystallogr E: Crystallogr Commun 72: 463-466.

Berenbaum MR (1981) Patterns of furanocoumarin distribution and insect herbivory in the Umbelliferae: plant chemistry and community structure. Ecology (62): 1254-1266.

Berenbaum MR (1983) Coumarins and caterpillars: a case for coevolution. Evolution 37:163-179.

Berenbaum MR (1990) Evolution of specialization in insect-umbellifer associations. Ann Rev Entomol 35: 319-342.

Berenbaum MR (1991) Coumarins. In: Rosenthal G, Berenbaum MR (ed) Herbivores their interactions with secondary plant metabolites. NY: Academic Press pp 221-224.

Berenbaum MR (1991b). Comparative processing of allelochemicals in the Papilionidae (Lepidoptera). Arch Insect Biochem Physiol 17: 213-221.

Berenbaum MR (1995) Phototoxicity of plant secondary metabolites: insects and mammalian perspectives. Arch Insect Biochem Physiol 29: 119-134.

Berenbaum MR, Favret C, Schuler MA (1996) On defining “key innovations” in an adaptive radiation: cytochrome P450S and Papilionidae. Am Naturalist 148: S139-S155.

Berenbaum MR, Zangerl AR (1991) Acquisition of a native hostplant by an introduced oligophagous herbivore. Oikos 62:153-159.

Berenbaum MR, Zangerl AR (1992) Genetics of physiological and behavioral resistance to host furanocoumarins in the parsnip webworm. Evolution 46:1373-1384.

Berenbaum MR, Zangerl AR (1998) Chemical phenotype matching between a plant and its insect herbivore. Proc Natl Acad Sci USA 95:13743–13748.

Berenbaum MR, Zangerl AR (2006) Parsnip webworms and host plants at home and abroad: trophic complexity in geographic mosaic. Ecology 87: 3070-3081.

Berenbaum MR, Zangerl AR, Lee K (1989) Chemical barriers to adaptation by a specialist herbivore. Oecologia 80: 501-506.

Berenbaum MR, Zangerl AR, Nitao JK (1986) Constraints on chemical coevolution; wild parsnips and the parsnip webworm. Evolution 40:1215-1228.

Brower AVZ (1994) Rapid morphological radiation and convergence among races of the butterfly *Heliconius erato* inferred from patterns of mitochondrial DNA evolution. Proc Natl Acad Sci USA 91:6491–6495.

Bouckaert R, Drummond A (2017) bModelTest: Bayesian phylogenetic site model averaging and model comparison. BMC Ecol Biol 17:42.

Bouckaert R, Vaughan TG, Barido-Sottani J, Duchêne S, Fourment M, Gavryushkina A, Heled J, Jones G, Kühnert D, de Maio N, Matschiner M, Mendes FK, Müller NF, Ogilvie HA, du Plessis L, Popinga A, Rambaut A, Rasmussen D, Siveroni I, Drummond AJ (2019) BEAST 2.5: An advanced software platform for Bayesian evolutionary analysis. PLoS Comput Biol 15(4): e1006650.

Bruni R, Barreca D, Protti M, Brighenti V, Righetti L, Anceschi L, Mercolini L, Benvenuti S, Gattuso G, Pellati F (2019) Botanical sources, chemistry, analysis, and biological activity of furanocoumarins of pharmaceutical interest. Molecules 24: 2163.

Bucheli SR, Passoa S, Wenzel JW (2010) A phylogenetic test of Ehrlich and Raven's theory of escape and radiation in insects that feed on toxic plants, based on Nearctic *Depressaria* moths (Gelechioidea: Elachistidae: Depressariinae), with discussion of the evolution of genitalia. Entomol Am 116: 1–24.

Calla B, Wu WY, Dean CAE, Schuler MA, Berenbaum MR (2020). Substrate-specificity of cytochrome P450-mediated detoxification as an evolutionary strategy for specialization on furanocoumarin-containing hostplants: CYP6AE89 in parsnip webworms. Insect Mol Biol 29: 112–123.

Carroll MJ (2003) Effects of dietary lutein on the parsnip webworm, *Depressaria pastinacella* (Lepidoptera: Elachistidae). Dissertation, University of Illinois Urbana-Champaign.

Clarke JF (1941) Revision of the North American moths of the family Oecophoridae: with descriptions of new genera and species. Proc US Nat Mus 90: 33-286.

Clarke JF (1952) Host relationships of moths of the genera *Depressaria* and *Agonopterix*: with descriptions of new species. Smithson Misc Collect 117: 1-20.

Crankshaw DL, Hetnarski K, Wilkinson CF (1979) Purification and characterization of NADPH-cytochrome C reductase from the midgut of the southern armyworm (*Spodoptera eridania*). Biochem. J. 181: 593– 605.

Dhar P, Heckler I, Garcia A, Santos J (2014) Phytochemical analysis and extraction/isolation and characterization of a new furanocoumarin from *Heracleum maximum*. Planta Med 80: PD65.

Ehrlich PR, Raven PH (1964) Butterflies and plants: A study in coevolution. Evolution 18: 586-608.

Fetz R (1994) Larval morphologische Beitrage zum phylogenetischen System der ehemaligen Oecophoridae (Lepidoptera, Gelechioidea). Neue Entomologische Nachrichten 33: 1–273.

Hannemann HJ (1995) Kleinschmetterlinge oder Microlepidoptera IV. Flachleibmotten (Depressariidae). Die Tierwelt Deutschlands, 69. Teil. G.Fischer Verlag, Jena, Stuttgart. 192 pp.

Harrison T, Dean CAE, Parks K, Berenbaum MR (2016) *Depressaria depressana* (Fabricius) (Depressariidae), new to the Midwestern USA. J Lepid Soc 70:169–173.

Hodges RW (1974) The moths of America north of Mexico. London, England.

Katoh K, Standley DM (2013) MAFFT Multiple sequence alignment software version 7: improvements in performance and usability. Mol Biol Evol 30:772–780.

Karsholt O, Razowski J (1996) The Lepidoptera of Europe: A distributional checklist. Apollo Books, Stenstrup, Denmark, 380 pp.

Krone W (1911) Neubeschreibungen einiger Arten und Varietäten von Microlepidopteren. Jahresbericht des Wiener Entomologischen Vereins 21: 39-42.

Landry JF, Nazari V, Dewaard JR, Mutanen M, Lopez-Vaamonde C, Huemer P, Hebert PD (2013) Shared but overlooked: 30 species of Holarctic Microlepidoptera revealed by DNA barcodes and morphology. Zootaxa, 3749: 1–93.

Lanfear R, Calcott B, Ho SYW, Guindon S (2012) PartitionFinder: Combined selection of partitioning schemes and substitution models for phylogenetic analyses. Mol Biol Evol 29: 1695–1701.

Loxdale HD, Harvey, JA (2016) The ‘generalism’ debate: misinterpreting the term in the empirical literature focusing on dietary breadth in insects. Biol J Linnean Soc (119): 265–282.

Mao W, Berhow MA, Zangerl AR, Mcgovern J, Berenbaum MR (2006). Cytochrome P450-mediated metabolism of xanthotoxin by *Papilio multicaudatus*. J Chem Ecol 32: 523–536.

McKenna DD, Berenbaum MR (2003) A field investigation of *Depressaria* (Elachistidae) Host plants and ecology in the Western United States. J Lepid Soc 57: 36-42.

Nitao JK, Berenbaum MR (1988) Laboratory rearing of the parsnip webworm, *Depressaria pastinacella* (Lepidoptera: Oecophoridae). Ann Entomol Soc Am 81: 485-487.

O'Neil T, Johnson JA, Webster D, Gray CA (2013) The Canadian medicinal plant *Heracleum maximum* contains antimycobacterial diynes and furanocoumarins. J Ethnopharmacol 147: 232-237.

Ovsyannikova EI, Grichanov IYa (2021) *Depressaria depressana* (F.) - Purple Carrot-seed Moth. Interactive Agricultural Ecological Atlas of Russia and Neighboring Countries. Economic Plants and their Diseases, Pests and Weeds. http://www.agroatlas.ru/en/content/pests/Depressaria_depressana/index.html. Accessed 28 March 2021.

Palm E (1989) [Oecophoridae (Lepidoptera) of northern Europe – With Special Reference to Denmark]. Danmarks Dyreliv Vol. 4. Apollo Books, Stenstrup. 247 pp. [in Danish]

Passoa SC (1995) Larval and pupal systematics of nearctic Amphisbatinae and Depressariinae (Lepidoptera: Oecophoridae). Dissertation, University of Illinois Urbana-Champaign.

Requena E, Joaquim J, De-Gregorio P (2014). Contribució al coneixement del gènere *Depressaria* Haworth, 1812 a Catalunya i Espanya (Lepidoptera: Depressariidae). Butll Soc Cat Lep 105: 13–30.

Rambaut A, Drummond AJ, Xie D, Baele G, Suchard MA (2018) Posterior summarization in Bayesian phylogenetics using Tracer 1.7. Syst Biol 67: 901–904.

Ratnasingham S, Hebert PD (2007) bold: The Barcode of Life Data System (http://www.barcodinglife.org). Mol Ecol Notes 7:355–364.

Rothwell EM, Holeski LM (2020) Phytochemical defences and performance of specialist and generalist herbivores: a meta-analysis. Ecol Entomol 45: 396–405.

Safar M, Lin BJ, Chen WH, Langauer D, Chang JS, Raclavska H, Pétrissans A, Rousset P, Pétrissans M (2019) Catalytic effects of potassium on biomass pyrolysis, combustion and torrefaction. Appl Energy 235: 346–35.

Sarker SD, Nahar, L (2017) Progress in the chemistry of naturally occurring coumarins. Progress in the chemistry of organic natural products 106: 241-304.

Scriber JM, Feeny P (1979) Growth of herbivorous caterpillars in relation to feeding specialization and to the growth form of their food plants. Ecology 60: 829-850.

Smilanich AM, Fincher RM, Dyer LA (2016) Does plant apparency matter? Thirty years of data provide limited support but reveal clear patterns of the effects of plant chemistry on herbivores. New Phytol 210: 1044–1057.

Sperling FA, Feeny P (1995) Umbellifer and composite feeding in *Papilio*: Phylogenetic frameworks and constraints on caterpillars. In: Scriber JM, Tsubaki Y, Lederhouse RC. Swallowtail butterflies: Their ecology and evolutionary biology. Scientific Publishers, Gainesville, Florida, pp 299-306.

Stamatakis A (2014) RAxML version 8: A tool for phylogenetic analysis and post-analysis of large phylogenies. Bioinformatics 30: 1312–1313.

Thompson JN, Price PW (1977) Plant plasticity, phenology, and herbivore dispersion: wild parsnip and the parsnip webworm. Ecology 58: 1112-1119.

Waldbauer GP (1968) The consumption and utilization of food by insects. Adv In Insect Phys (5): 229-288.

Walsingham, Lord T De G (1881) On some North-American Tineidae. P Zool Soc London 1881:301-325.

Wieser C, Huemer P (1997) Bemerkenswerte Nachweise von Schmetterlingen aus kärnten (Lepidoptera). Carinthia 187: 385-393.

Yu Y, Blair C, He X (2020) RASP 4: ancestral state reconstruction tool for multiple genes and characters. Mol Biol Evol 37: 604–606.

Zobel AM, Brown SA (1990) Dermatitis-inducing furanocoumarins on leaf surfaces of eight species of rutaceous and umbelliferous plants. J Chem Ecol 16: 693-700.

CHAPTER 2

NINA-B EXPRESSION ASSOCIATED WITH β-CAROTENE CONSUMPTION IN THREE LEPIDOPTERANS WITH FURANOCOUMARIN-CONTAINING HOSTPLANTS

INTRODUCTION

In animals, carotenoids are involved in antioxidant defense (Felton and Summers 1995), color pattern development (Hill 1991), immune system activation (Von Lingtig 2010), and vision development (Gu et al. 2004). However, because they cannot synthesize carotenoids endogenously, animals typically obtain carotenoids through their diet (Britton et al. 2004). Although carotenoid uptake, metabolism, and sequestration have been widely studied in vertebrates, particularly with respect to the striking color patterns of birds and lizards, the genetic mechanisms underlying these processes are less well-known (Toews et al. 2018). Investigations of the dietary uptake of carotenoids in insects, however, have provided many of the fundamental insights into the molecular basis of carotenoid metabolism and sequestration (Heath et al. 2013).

In the case of vision development, *Drosophila melanogaster* has been used as a model to demonstrate experimentally that β-carotene is metabolized by an isomerooxygenase enzyme, encoded by *ninaB*, and sequestered, in part, by the activity of a scavenger receptor protein class B type 1 (SR-BI) encoded by *ninaD* (Voolstra et al. 2006; Oberhauser et al. 2008). This activity is necessary for the biosynthesis of the 3-hydroxyl chromophore of rhodopsin (Gu et al. 2004, Yang and O'Tousa 2007) linked to the photodetection that initiates diapause induction (Toews et al. 2017). With respect to sequestration, mutations in *scrb15* and *cameo2*, which code for receptors involved in the deposition of lutein (as well as other xanthophylls) and β-carotene,

respectively, were identified as causing aberrant color pattern morphs of the pupal cocoons of *Bombyx mori* larvae raised on mulberry leaves with high carotenoid content; like *ninaD, scrb15* encodes a class B scavenger receptor (Tsuchida and Sakudoh 2015).

As is the case with other animals, carotenoids play an important role in protecting against reactive oxygen species. Beta-carotene is an effective antioxidant with a high capacity for quenching singlet oxygen (Perez-Galvez et al. 2020). This quenching ability may contribute to the protective effects of dietary β-carotene against the toxic effects of photoactivated alpha-terthienyl in tobacco hornworm (*Manduca sexta)* larvae (Aucoin et al. 1990); similarly, the presence of α-carotene and β-carotene stores in the larval midgut of several polyphagous *Spodoptera* species increased survivorship on leaves of the toxic plant lima bean (*Phaseolus lunatus*) (Shao et al. 2011), although *P. lunatus* is not known to be phototoxic.

Another example of carotenoid sequestration as a mechanism for relieving oxidative stress associated with phototoxic food is lutein sequestration by the parsnip webworm, *Depressaria radiella* (Lepidoptera: Depressariidae), an invasive web-building caterpillar of Eurasian origin. The major North American hostplant for this insect is the wild parsnip, *Pastinaca sativa* (Carroll et al. 1997; Carroll 2003), an invasive weed from Europe. The relationship between *D radiella* and *P. sativa* has been described as a coevolutionary arms race, whereby the plants defend themselves by synthesizing photoactive toxic furanocoumarins, which *D. radiella* metabolizes, in part, through substrate- specific cytochrome P450s monooxygenases (P450s) (Berenbaum and Zangerl 1992; Wu et al. 2004; Mao et al. 2006). Furanocoumarins prevent replication of DNA and RNA by binding to pyrimidine bases (Dall'Acqua 1978). The photogenotoxic effects of furanocoumarins occur in the presence of ultraviolet light, which activates the conversion of furanocoumarins from ground state to the triplet state, in which form

they can either react with DNA and RNA directly or with ground state oxygen molecules to produce singlet oxygen, superoxide anion, and hydroxyl radicals. Both reactions can incur cellular damage by denaturing proteins, disrupting lipids, and damaging other non-target molecules (Berenbaum 1991).

In addition to metabolic adaptation to phototoxic furanocoumarins, the parsnip webworm sequesters lutein, a xanthophyll that appears to function as a form of physiological resistance to furanocoumarins. Carroll et al. (1997) determined that the characteristic yellow stripe along the underside of ultimate instar *D. radiella* larvae consuming the yellow flowers of *P. sativa* is derived from sequestered lutein, along with other xanthophylls. In the laboratory, these caterpillars avoid UVA light when fed a carotenoid-free diet containing xanthotoxin, a phototoxic furanocoumarin, but this behavior is eliminated when their diet is supplemented with lutein, suggestive of a protective function of the sequestered pigment. Carroll (2003) demonstrated that dietary lutein reduced the toxic effects of high concentrations of xanthotoxin in *D. radiella*, as measured by survivorship assays and gravimetric estimates of growth and development.

Whether other lepidopterans associated with phototoxic furanocoumarins similarly depend on carotenoid pigment-based defenses is unknown. Ultimate instar larvae of the purple carrot seed moth (*Depressaria depressana*), a congener of *D. radiella* of Eurasian origin recently introduced to North America (Harrison et al. 2016), is reddish-purple in color and lacks a yellow stripe. While it also utilizes *P. sativa* as a major hostplant, *D. depressana* has a broader host range than that of *D. radiella*, with host records encompassing species in at least a dozen genera from five different tribes within the Apiaceae (Chapter 1), including plants that produce furanocoumarins in negligible quantities, such as *Daucus carota* (wild carrot) (Harrison et al.

2016; Khalil et al. 2018). Outside the family Depressariidae, the cabbage looper, *Trichoplusia ni* (Lepidoptera: Noctuidae), exhibits a broadly polyphagous feeding strategy across multiple plant families, occasionally including some species in the Apiaceae (Leite-Mondin et al. 2021). *T. ni* larvae sequester both unmodified β-carotene and xanthophylls (including lutein) at higher concentrations than are present in hostplant tissues, irrespective of plant species identity (Nguyen et al. 2019), but whether this carotenoid sequestration protects the larvae from photooxidative damage has not been examined.

On the basis of previous research demonstrating that dietary β-carotene reduces the toxic effect of photooxidative furanocoumarins in at least one lepidopteran, I measured the expression of *ninaB* in three lepidopterans differentially dependent on furanocoumarin-containing plants in the presence and absence of furanocoumarins. Quantitative real-time PCR was used to measure expression of this gene in *D. radiella, D.depressana,* and *T. ni* when larvae consumed diets containing either xanthotoxin (a frequently encountered linear furanocoumarin), β-carotene, or both compounds together.

METHODS

Insects

To obtain *D. radiella* for bioassays, eggs from a source population with *P. sativa* as the sole available hostplant were collected from the abaxial surfaces of leaves at Phillips Tract, an oldfield maintained by University of Illinois Urbana-Champaign (UIUC) in central Champaign County (40.12966, -88.14390). Larvae were reared to ultimate instar under laboratory conditions prior to experimentation individually in 30-ml Solo® cups containing 5 g of fresh semi-defined artificial diet (hereafter, artificial diet) prepared using a recipe outlined in Nitao and Berenbaum

(1988). Laboratory colonies were maintained at 27 ± 4ºC and exposed to a 16:8 L:D photoperiod.

Multiple instars of *Depressaria depressana* were collected from the umbels of either *P. sativa* or *D. carota* at Phillips Tract. In the laboratory, larvae were reared through to adulthood on artificial diet and allowed to mate and lay eggs. Adults were then placed in 950-ml deli cups containing a 100-ml tube plugged with a cotton dental wick filled with a 50% honey water solution, which was used as a food source. This enclosure also contained green filter paper impregnated with an extract of *P. sativa* leaves in 70% EtOH, simulating hostplant foliage for oviposition (Nitao and Berenbaum 1988). Eggs were individually collected from the filter paper and transferred to new 30-ml Solo® cups containing fresh on the same artificial diet prepare for parsnip webworms. Ultimate instar *D. depressana* larvae of the subsequent generation were used for assays.

Third instar larvae of *Trichoplusia ni* were purchased from Benzon Research Inc. (Carlisle, PA). Upon arrival, larvae were individually transferred to new 30-ml Solo® cups containing fresh artificial diet prepared in the same way as both *Depressaria* species, where they were reared to ultimate instars before being collected for use in assays.

For bioassays, ten ultimate instar larvae of each species were individually placed in new 30-ml Solo® cups, each containing one of four diets: unsupplemented artificial diet (AD), 1% xanthotoxin in artificial diet (1% Xan), 1% β-carotene in artificial diet (1% β-caro), or 1% xanthotoxin and 1% β-carotene in artificial diet (1% Xan + 1% β-caro). Larvae were allowed to feed *ad libitum* for three days before being collected on Day 4 and flash-frozen in liquid nitrogen prior to tissue homogenization via mortar and pestle (Fisher Scientific, Hampton, NH).

Sample Processing

Total RNA was isolated with the Machery-Nagel Nucleospin RNA Kit following the manufacturer's instruction manual (Machery-Nagel, Allentown, PA) with the following adjustment: cell lysis occurred in a solution of 3 µl of 1.0 M DTT mixed in 300 µl of buffer RA1. Genomic DNA was eliminated from the sample via incubation for 15 minutes using 95 µl DNAse I solution. RNA was eluted in 30 µl molecular grade water. RNA concentration was assessed via Nanodrop spectrophotometer (Thermo Fisher Scientific, Waltham, Massachusetts). Preparation of double-stranded cDNA was performed using the NEB Protoscript II (New England Biolabs, Ipswich, MA) kit following the manufacturer's instruction manual. First-strand cDNA synthesis reactions consisted of 500 ng total RNA in 5ul total volume, 1 µl oligo(dT) primer, 1 µl 10 mM dNTP mix, and 3 µl DEPC-treated water.

Real-time Quantitative PCR

Standard 96-well plates were used to perform qPCR, each of which contained cDNA for each sample loaded in triplicate, no-template controls, and pooled cDNA at serially diluted concentrations of 1, 1:10, 1:100, 1:1,000, 1:10,000. Actin was used as the housekeeping control gene for this experiment. *Actin* and *ninaB* primers for all three species are presented in Table 2.1. For qPCR reactions, Luna Universal qPCR Master Mix (New England Biolabs, Ipswich, MA) was used and each reaction mixture consisted of 5 µl Luna master mix, 1 µl forward and reverse primers, 2 µl H_2O, and 2 µl cDNA template. Reactions were run with the following temperature cycle: 95ºC/1 min for the initial denaturation phase, then 40 cycles of 95ºC/15 s, 60ºC/30 s, 95ºC/15 s, followed by a final extension phase at 60ºC/1 min in an Applied Biosystems StepOnePlus (Thermo Fisher Scientific, Waltham, MA).

qPCR Data Analysis

Gene expression was calculated using the ΔΔCt method. The Ct (critical threshold value) of the reference gene, *actin*, was subtracted from the Ct of *ninaB* to obtain the ΔCt. *Actin* was selected as the reference gene because, due to its stable expression levels, it has previously been successfully used for qPCR in *D. radiella* (Li et al. 2004). The relative fold change (ΔΔCt) for each treatment group was obtained by dividing the mean relative expression value of each treatment group by the mean expression of the control group. A Shapiro-Wilks test and a Levene-Forsythe test were implemented to check assumptions of normality and homogeneity of variance, respectively. Statistically significance differences between treatment means were assessed via analysis of variance (ANOVA) with a post-hoc Tukey's test in R v. 4.1.0 as implemented in Rstudio version 1.1.419 (Boston, MA).

RESULTS

Across the three lepidopterans in this study, all responded similarly to phytochemical additions to the artificial diet in terms of transcriptional regulation of *ninaB*; relative to larvae in control groups, which consumed unsupplemented artificial diet, larvae in all experimental treatments displayed significantly downregulated expression of *ninaB* (ANOVA, Tukey, $P < 0.05$) (Fig 2.1). In *D. radiella* (Fig.1.1A), across the three experimental treatments, downregulation was most pronounced on the diet containing only 1% xanthotoxin (Fig 2.1); supplementation of the diet with 1% β-carotene reduced downregulation in both the presence and absence of xanthotoxin. By contrast, in *D. depressana*, all four diets produced expression levels significantly different from one another, with larvae consuming 1% Xan + 1% β-caro diet showing the greatest downregulation (ANOVA, Tukey, $P < 0.05$) (Fig 2.1B), larvae on the 1%

xanthotoxin diet the least downregulation, and larvae on the 1% β-Caro diet displaying an intermediate degree of downregulation of *ninaB* relative to the control in *D. depressana* (ANOVA, Tukey, $P < 0.05$) (Fig 2.2). Finally, in *T. ni,* all three experimental diets resulted in significantly downregulated expression of *ninaB* relative to the unsupplemented artificial diet (ANOVA, Tukey, $P < 0.05$) (Fig 2.3). Larvae on diets containing either 1% Xan or 1% β-Caro displayed significant downregulation relative to the 1% Xan + 1% β-caro treatment (ANOVA, Tukey, $P < 0.05$) (Fig 2.3).

DISCUSSION

Across all trials, consumption of xanthotoxin or β-carotene, either separately or in combination, resulted in significantly downregulated expression of *ninaB*. In the three species in this study, *ninaB* was significantly downregulated across all three experimental diets relative to the unsupplemented control group, thus providing preliminary evidence that enzymatic cleavage of β-carotene is reduced in the presence of xanthotoxin. However, across the three species tested, there was no consistent pattern as to which experimental treatment elicited the greatest downregulation of *ninaB*. These differences may reflect differences across the species in their degree of specialization for consuming plant tissues containing phototoxic furanocoumarins. While sequestration of dietary lutein in *D. radiella* is well documented with respect to color pattern development (Carroll and Berenbaum 2006), behavioral modifications (Carroll et al. 1997), and protection against furanocoumarins (Carroll 2003), the genetic mechanisms underlying sequestration and usage of β-carotene in this species require further elucidation. In other insect species, *ninaB* encodes β-carotene-15,15'-oxygenase, which catalyzes the centric

cleavage of β-carotene (Yang 2006). Consumption of β-carotene in the diet appears to mitigate the downregulation of *ninaB* in *D. radiella* and in *T. ni* (Fig. 2.1).

In contrast, downregulation of *ninaB* in *D. depressana* is more apparent in diets containing β-carotene (Fig. 2.2). By reducing the production of β-carotene-15,15'-oxygenase, sequestration of unmodified β-carotene is likely promoted at a higher rate than in *D. radiella* when exposed to xanthotoxin. Owing to its broader range of hostplants relative to *D. radiella* (Chapter 1), exposing *D. depressana* to a greater diversity of plant chemical defense profiles, this species may rely more on antioxidants such as β-carotene as a compensatory mechanism to overcome a lack of highly efficient specialized P450s that detoxify furanocoumarins (Chapter 3). Further examination of enzymes facilitating the cellular transport and uptake of β-carotene is needed to elucidate its role in antioxidant defense against dietary phototoxic compounds in *D. depressana*. Another gene that warrants investigation is *ninaD*, which codes for Scavenger Receptor Class B (Yang and O'Tousa 2007). This receptor has been identified as a β-carotene specialist in *Drosophila melanogaster* (Yang and O'Tousa 2007) and in *Bombyx mori* (renamed *scrb15*) (Tsuchida and Sakudoh 2015). These studies examined the expression of *ninaD* in the context of visual development and pupal coloration, respectively, and its expression in response to dietary furanocoumarins remains unknown.

In the case of *T. ni*, the downregulation of *ninaB* is greatest in diets containing either xanthotoxin or β-carotene but this downregulation is decreased in the diet containing both compounds (Fig. 2.3). Whereas *T. ni* is recorded to feed upon more than 100 plant species (Leite-Mondin et al. 2021), it rarely encounters dietary furanocoumarins in its hosts (Timmermann et al. 1999), as reflected by its relatively low survivorship when experimentally exposed to xanthotoxin (Zangerl 1990). As such, the possibility that the expression of *ninaB* and therefore

sequestration of β-carotene may not be correlated with ingestion of xanthotoxin cannot be discounted. Unmodified β-carotene was previously found to be sequestered in the midgut of larval *T. ni*, which obtained this carotenoid from two hostplants tested, *Lactuca sativa* var. *longifolia* and *Brassica oleracea* var *sabellica*, and used as a precursor for hormone synthesis and antioxidant defense (Nguyen et al. 2019). Additionally, increased presence of dietary β-carotene positively affects growth rate and immunological responses, such as melanization of pathogens (Clark and Lampert 2018). Outside of its immunological properties, sequestration of unmodified β-carotene, among other carotenoids, is also integral to the cryptic coloration of *T. ni* (Welch et al. 2017). *T. ni* is not known to use other antioxidants as defense protection against xanthotoxin (Timmermann et al. 1999), so it may make similar use of β-carotene.

Carotenoids such as lutein and β-carotene are ubiquitous in most higher plant taxa (Seki and Vogt 1998), where they are indispensable agents of protection against oxidative stress during the process of photosynthesis. Herbivorous insects in a range of taxa appear to have coopted these pigments to serve as adjuncts to specialized enzymatic activity, as in the case of *D. radiella* and its P450-mediated detoxification of furanocoumarins (Carroll 2003), or generalized antioxidant repair of damaged tissues as in the case of *T. ni* (Ahmad and Pardini 1990). Results of my study suggests that *ninaB* warrants further investigation from the scientific community, particularly in herbivorous insects, as its physiological activity appears to extend beyond rhodopsin production and vision development.

TABLE AND FIGURE

Table 2.1 Primers used in the present study.

Gene	Direction	Primer Sequence	Species
Actin	Forward	5’ CCAGTGGAAGACTGTGATCCATATCC 3’	All
	Reverse	5’ GAGAGCGCCTGTTATCTATTATCTCC 3’	
NinaB	Forward	5’ GCCAGTGGCTAAATGTTGGC 3’	*D. radiella*
	Reverse	5’ GATTCATCGAAATCGGAGCGT 3’	
NinaB	Forward	5’ GCCAGTGGCTAAATGTTGGC 3’	*D. depressana*
	Reverse	5’ GATTCATCGAAATCGGAGCGT 3’	
NinaB	Forward	5’ CAGGTGAATTTCCGTCATGGC 3’	*T. ni*
	Reverse	5’ ACTGGTACGTCACTGTGCC 3’	

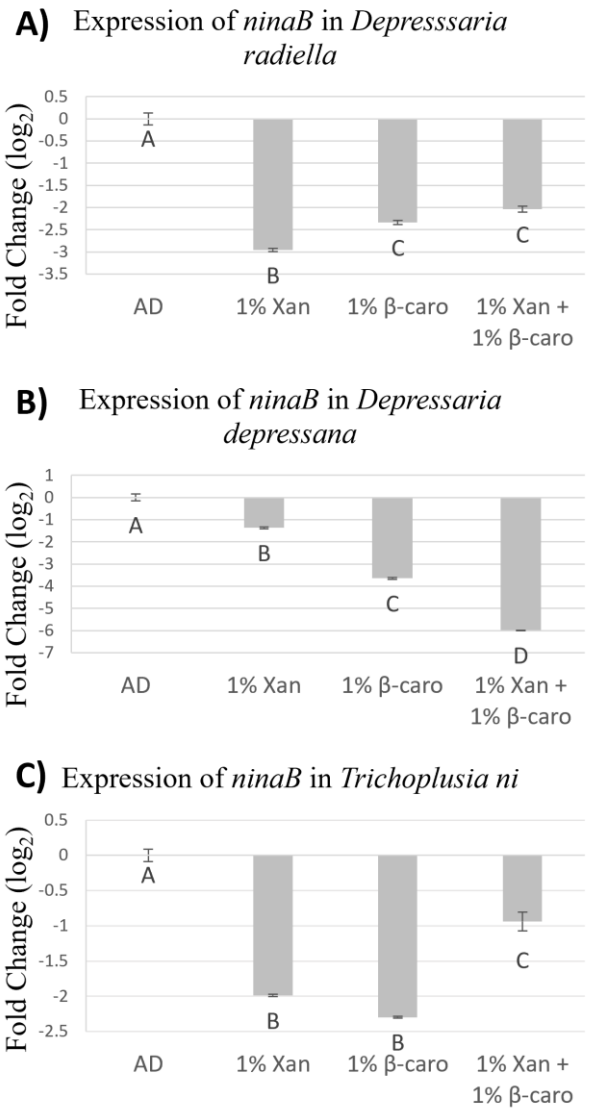

Figure 2.1 Expression of *ninaB* transcripts in ultimate instars of (A) *Depressaria radiella*, (B) *Depressaria depressana*, and (C) *Trichoplusia ni* after 3d of feeding on either unsupplemented semi-defined artificial diet (AD), 1% xanthotoxin in artificial diet (1% Xan), 1% β-carotene in artificial diet (1% β-caro), or 1% xanthotoxin and 1% β-carotene in artificial diet (1% Xan + 1% β-caro). Fold change was calculated via ΔΔCt method before being log transformed. Bars indicate the mean $\pm$ SE. Letters denote significant differences (ANOVA, Tukey HSD, $P > 0.05$) post hoc comparisons.

REFERENCES

Ahmad S, Pardini RS (1990) Mechanisms for regulating oxygen toxicity in phytophagous insects. Free Radic Biol. 8:401-413.

Aucoin RR, Fields P, Lewis MA, Philogene BJR, Arnason JT (1990) The protective effect of antioxidants to a phototoxin-sensitive insect herbivore, *Manduca sexta*. J Chem Ecol 16: 2913–2924.

Berenbaum MR (1983) Coumarins and caterpillars: a case for coevolution. Evolution 37: 163-179.

Berenbaum MR (1991) Coumarins. In: Rosenthal G, Berenbaum MR (ed) Herbivores Their Interactions with Secondary Plant Metabolites. NY: Academic Press pp 221-249.

Berenbaum MR, Zangerl AR (1991) Acquisition of a native hostplant by an introduced oligophagous herbivore. Oikos 62: 153-159.

Berenbaum MR, Zangerl AR (1992) Genetics of physiological and behavioral resistance to host furanocoumarins in the parsnip webworm. Evolution 46: 1373-1384.

Berenbaum MR, Zangerl AR, Nitao JK (1986) Constraints on chemical coevolution; wild parsnips and the parsnip webworm. Evolution 40: 1215-1228.

Britton G, Liaaen-Jensen S, Pfander H (2004) Carotenoids Handbook. Birkhaüser Verlag, Boston, MA.

Carroll MJ (2003) Effects of dietary lutein on the parsnip webworm, *Depressaria pastinacella* (Lepidoptera: Elachistidae). Dissertation, University of Illinois Urbana-Champaign.

Carroll M, Hanlon A, Hanlon T, Zangerl AR, Berenbaum MR (1997) Behavioral effects of carotenoid sequestration by the parsnip webworm, *Depressaria pastinacella*. J Chem Ecol 23: 2707-2719.

Clark KA, Lampert E (2018) Effects of dietary β-carotene on the melanization response and growth rate of *Trichoplusia ni* (Lepidoptera: Noctuidae). Environ Entomol 47: 1618-1622.

Dall 'Acqua F, Vedaldi D, Recher M (1978) The photoreaction between furocoumarins and various DNA with different base compositions. Photochem Photobiol 27: 33-36.

Felton GW, Summers CB (1995). Antioxidant systems in insects. Arch Insect Biochem Physiol 29: 187-197.

Gu G, Yang J, Mitchell KA, O'Tousa JE (2004) *Drosophila* NinaB and NinaD act outside of retina to produce rhodopsin chromophore. JBC 279: 18608–18613.

Harrison T, Dean CAE, Parks K, Berenbaum MR (2016) *Depressaria depressana* (Fabricius) (Depressariidae), new to the Midwestern USA. J Lepid Soc 70: 169–173.

Heath JJ, Cipollini DF, Stireman JO (2013) The role of carotenoids and their derivatives in mediating interactions between insects and their environment. Arthropod-Plant Interact 7: 1-20.

Hill GE (1991) Plumage coloration is sexually selected indicator of male quality. Nature 350: 337–340.

Leite-Mondin M, DiLegge MJ, Manter DK, Weir TL, Silva-Filho MC, Vivanco JM (2021) The gut microbiota composition of *Trichoplusia ni* is altered by diet and may influence its polyphagous behavior. Sci Rep 11: 1.

Li W, Zangerl AR, Schuler MA, Berenbaum MR (2004) Characterization and evolution of furanocoumarin-inducible cytochrome P450s in the parsnip webworm, *Depressaria pastinacella*. Insect Mol Biol 13: 603-613.

Nguyen KO, Al-Rashid S, Clarke Miller M, Tom Diggs J, Lampert EC (2019) *Trichoplusia ni* (Lepidoptera: Noctuidae) Qualitative and quantitative sequestration of host plant carotenoids. Environ Entomol 48: 540–545.

Nitao JK, Berenbaum MR (1988) Laboratory rearing of the parsnip webworm, *Depressaria pastinacella* (Lepidoptera: Oecophoridae). Ann Entomol Soc Am 81: 485-487.

Oberhauser V, Voolstra O, Bangert A, von Lintig J, Vogt K (2008) NinaB combines carotenoid oxygenase and retinoid isomerase activity in a single polypeptide. PNAS 105: 19000-19005.

Seki T, Vogt K (1998) Evolutionary aspects of the diversity of visual pigment chromophores in the class Insecta. Comp Biochem Physiol B 119: 53- 64.

Shao Y, Spiteller D, Tang X, Ping L, Colesie C, Münchberg U, Bartram S, Schneider B, Büdel B, Popp J, Heckel DG, Boland W (2011) Crystallization of α- and β-carotene in the foregut of *Spodoptera* larvae feeding on a toxic food plant. Insect Biochem Mol Biol, 41: 273–281.

Timmermann SE, Zangerl AR, Berenbaum MR (1999). Ascorbic and uric acid responses to xanthotoxin ingestion in a generalist and a specialist caterpillar. Arch Insect Biochem Physiol 42: 26-36.

Toews DPL, Hofmeister NR, Taylor SA (2017) The evolution and genetics of carotenoid processing in animals. Trends Genet 33: 171–182.

Tsuchida K, Sakudoh T (2015) Recent progress in molecular genetic studies on the carotenoid transport system using cocoon-color mutants of the silkworm. Arch Biochem Biophys 572: 151–157.

Welch BJ, Obadi OM, Lampert EC (2017) Effects of carotenoid sequestration on a caterpillar's cryptic coloration and susceptibility to predation. Entomol Exp Appl 163:177-83.

Yang J, O'Tousa JE (2007) Cellular sites of *Drosophila* NinaB and NinaD activity in vitamin A metabolism. Mol Cell Neurosci 35: 49–56.

Young AJ, Lowe GM (2001) Antioxidant and prooxidant properties of carotenoids. Arch Biochem Biophys 385: 20-27.

Zangerl AR (1990) Furanocoumarin induction in wild parsnip: evidence for an induced defense against herbivores. Ecology 71: 1926-1932.

CHAPTER 3

TRANSCRIPTOMIC ANALYSIS AND CHARACTERIZATION OF CYTOCHROME P450 GENES MEDIATING FURANOCOUMARIN DETOXIFICATION IN THE PURPLE CARROT SEED MOTH (*DEPRESSARIA DEPRESSANA*) (LEPIDOPTERA: DEPRESSARIIDAE)

INTRODUCTION

Cytochrome P450 monooxygenases (P450s) are membrane-bound proteins structurally defined by a heme iron center; members of this enzyme superfamily perform a wide array of functions, including endogenous functions as biosynthesis and degradation of hormones and pheromones (Iga and Kataoka 2012) as well as such exogenous functions as metabolism of xenobiotic substrates (Nauen et al. 2021; Calla 2021). Detoxification reactions typically involve oxidation reactions whereby oxygen is added to lipophilic compounds to increase water solubility and facilitate excretion from the cell. This process, referred to as functionalization, is central to the Phase 1 stage of insect metabolism (Hoi et al 2014).

P450s are categorized into four clans: Clan 2, Clan 3, Clan 4, and Mitochondrial P450s (Amezian et al. 2021). Clan 2 P450s are highly conserved and are typically associated with steroid hormone synthesis. Mitochondrial P450s are also involved in the biosynthesis of steroid hormones. Because both Clan 2 and Mitochondrial P450s perform highly conserved functions, their numbers do not vary much even across insect orders and their conserved structural features facilitate identification of orthologs across many species. The major function of Clan 3 P450s is the metabolism of xenobiotics. This clan is highly variable across insect taxa as environmental selective pressures lead to ‘blooms’ following gene duplication events whereby P450s

proliferate, diversify, and acquire new functions. Clan 4 P450s perform a broad array of functions such as pheromone processing, lipid processioning, and detoxification (Feyereisen 2020). Insect CYPomes, the complete inventory of P450s present in the genome, differ greatly in size and whether this variation is a function of environmental selective pressures, random birth and death processes, or lineage stability remains a topic of discussion (Darragh et al. 2021).

The P450 mediated-detoxification of furanocoumarins by *Depressaria radiella* (Lepidoptera: Depressariidae) provides the basis of a model system of coevolved species. Specifically, *D. radiella* represents a highly specialized herbivore with a very limited number of hostplants—i.e., a "superspecialist," with a host range confined to a small number of closely related plant genera. This type of interaction has been reconstructed multiple times by virtue of accidental introductions from the native range of both species—Eurasia—into other parts of the world, including North America and New Zealand (Zangerl et al. 2008). In the USA, these introductions led to a reestablishment of a ditrophic association between the webworm and the subsequent convergent phenotype matching of its major hostplant wild parsnip, *Pastinaca sativa*, which produces large quantities of linear furanocoumarins as defenses against herbivores (Zangerl and Berenbaum 2003). In this system, both wild parsnip and parsnip webworms rely in part on P450 genes for phytochemical defense and detoxification, respectively; the amount of additive genetic variance in these traits may ultimately constrain the evolution of chemical phenotypes. As such, reestablishment of this plant-insect interaction across several continents has produced repeated instances of particular defensive compound and detoxification enzyme profiles (Berenbaum and Zangerl 2008; Zangerl and Berenbaum 2003; Zangerl et al. 2008).

Few specific P450 encoding genes have been functionally characterized as important in the detoxification of furanocoumarins in *D. radiella*; to date, these include CYP6AB3 for the

detoxification of imperatorin (Mao et al. 2006) and CYP6AE89 for the detoxification of xanthotoxin and isopimpinellin (Calla et al. 2020). Additionally, evidence suggests that CYP6AE1 is involved in the detoxification of the angular furanocoumarin sphondin (Li et al. 2004). Calla et al. (2017) annotated the entire *D. radiella* CYPome and found that the largest subfamilies in the CYPome, CYP6B, CYP6AB, CYP6AE, CYP9A, CYP9G, and CYP321, have been implicated in other lepidopterans in detoxification of xenobiotics. This pattern supports the hypothesis that, at least in the Clan 3 P450s, "blooms" increasing gene numbers and diversity may be driven at least in part by environmental selective pressures.

Whereas interactions between *D. radiella* and its hostplants are well studied, much less is known about the genetically encoded detoxification mechanisms of dietary furanocoumarins in a closely related congener, *Depressaria depressana*. Like *D. radiella*, this species is of Eurasian origin and specializes on plants belonging to the family Apiaceae. However, unlike *D. radiella*, which is a superspecialist that feeds almost exclusively on species in two genera in North America, *D. depressana* is a family-level specialist, which utilizes hostplants from multiple tribes within the Apiaceae. The preferred hosts of *D. depressana* include plants that produce furanocoumarins in abundance, such as *P. sativa*, as well as plants that produce low quantities, such as *Daucus carota* (Harrison et al. 2016). This species has recently been introduced to North America and is currently expanding its range west across the continent (Harrison et al. 2016), where it will likely encounter a variety of native umbellifers that could potentially function as suitable hosts. A better understanding of the evolutionary and ecological processes underlying the colonization of *D. depressana* is essential to predicting with greater accuracy its ability to incorporate novel hostplants into its diet. Specifically, characterizing transcriptional regulation of detoxification enzymes in response to ingested furancoumarins, as has been done in *D. radiella*

(Calla et al. 2017), would further resolve the biological idiosyncrasies of invasive species occupying difference spaces along the feeding strategy continuum. To that end, I used RNA-seq to elucidate differential gene expression, including CYP genes, in *D. depressana* corresponding to experimental diets containing the linear furanocoumarin xanthotoxin and the angular furanocoumarin sphondin, both of which occur in the two hostplant genera of *D. radiella*.

METHODS

D. depressana Sampling and Preparation

Populations of *D. depressana* were first recorded at Phillips Tract in 2015, with larvae observed feeding on umbels of *P. sativa* and *Daucus carota* (Harrison et al. 2016). *Depressaria depressana* larvae of varying instars were collected from the umbels of *P. sativa* at this location (40.12966, -88.14390) in June 2019. This site is an oldfield maintained by University of Illinois Urbana-Champaign in central Champaign County, Illinois. Individuals sampled from Phillips Tract were reared to adulthood and allowed to mate and lay eggs in the laboratory. Larvae were housed in 1-oz. (28 ml) Solo® cups lined with 5 g of semi-defined artificial diet (hereafter, artificial diet) (Nitao and Berenbaum 1988) and were allowed to feed *ad libitum*. Adults were relocated to 950-ml deli cups containing a 100-ml glass tube plugged with a cotton dental wick filled with a 50% honey water solution, which was used as a food source. This enclosure also contained green filter paper impregnated with 70% ethanolic extract of *P. sativa* leaves, providing a hostplant substitute suitable for oviposition (Nitao and Berenbaum 1988). Eggs were individually collected from the filter paper and transferred to new 30-ml deli cups containing fresh artificial diet. Ultimate instar *D. depressana* larvae of this subsequent laboratory-reared generation were sampled for analysis. Larvae were relocated to new Solo® cups containing one

of two experimental treatments: with diet supplemented with furanocoumarins--1% xanthotoxin in artificial diet or 0.02% sphondin in artificial diet. and unsupplemented artificial diet, which was used as the control. Larvae were allowed to feed for three days before being removed from the containers on Day 4 and flash- frozen in liquid nitrogen prior to tissue homogenization via mortar and pestle (Fisher Scientific, Hampton, NH).

Total RNA was isolated via Machery-Nagel Nucleospin RNA Kit (Machery-Nagel, Allentown, PA) following the manufacturer's instruction manual save for the several adjustments. Cell lysis occurred in a solution of 3 µl of 1.0 M DTT mixed in 300 µl of buffer RA1. Genomic DNA was eliminated from the sample via 15 minutes incubation using 95 µl DNAse I solution. RNA was eluted in 30 µl molecular grade water. RNA concentration and quality were assessed via a Nanodrop spectrophotometer (Thermo Fisher Scientific, Waltham, MA) and a Qubit fluorometer (Thermo Fisher Scientific, Waltham, MA). Preparation of cDNA libraries was performed using NEB Protoscript II kit following the manufacturer's instruction manual (New England Biolabs, Ipswich, MA). First-strand cDNA synthesis reactions consisted of 5 µl 500 ng total RNA, 1 µl oligo(dT) primer, 1 µl 10 mM dNTP mix, and 3 µl DEPC-treated water.

De Novo Transcriptome Assembly

Samples were sent to the Roy J. Carver Biotechnology Center at University of Illinois Urbana-Champaign (Urbana, Il) and sequenced via NovaSeq (Illumina, San Diego, CA). Sequencing generated more than a billion 150 nt paired end reads. Raw reads were trimmed using Trimmomatic (Bolger et al. 2014) and a de novo transcriptome was assembled using Trinity (Haas et al. 2013). Trimmed reads were mapped back to the assembled transcriptome and

transcript abundance was estimated and normalized using RSEM (Li and Dewey 2011). Open reading frames, coding sequences, and translations for all isoforms were predicted via Transdecoder (http://transdecoder.github.io). Functional annotation of transcripts was accomplished through the Trinotate annotation pipeline (Bryant et al. 2017) where homology of the generated transcripts to known sequences was first evaluated with BLAST (blastp) against the SwissProt database. Protein domain identification was assessed using PFAM, and protein signal and transmembrane domains were predicted using signalP and tmHMM, respectively.

Differential Expression Analysis

Statistical evaluation of differences in transcript abundance among samples was performed using the EdgeR package from the R-Bioconductor (Robinson et al. 2010).

Gene Ontology Enrichment Analysis

GO assignments were generated following the Trinotate protocol (Bryant et al. 2017). The Bioconductor package GOseq was used to perform functional term enrichment analysis. Differentially expressed genes identified using EdgeR were mapped using GO terms.

Identifying Cytochrome P450s

The Trinotate output report was searched for putative cytochrome P450s. Resulting candidate P450 assembled transcripts were then subjected to reciprocal best BLAST hit searches to assess orthology with cytochrome P450s in six other species of Lepidoptera with fully annotated CYPomes: *D. radiella* (Depressariidae), *Chilo suppressalis* (Pyralidae), *Amyelois transitella* (Pyralidae), *Trichoplusia ni* (Noctuidae), *Bombyx mori* (Bombycidae), and *Plutella*

xylostella (Plutellidae). Putative P450s were then sent to Dr. David R. Nelson (University of Tennessee) for official naming.

Lepidoptera P450 Phylogeny

A total of 588 cytochrome P450 protein sequences from the seven Lepidoptera, as well as a non-insect crustacean outgroup, *Daphnia pulex*, were compiled and aligned using hmmalign in the Hmmer suite (hmmer.org). A model specific to cytochrome P450 sequence alignment (p450: PF00067) was implemented for this alignment. The full CYPome phylogeny was constructed in Geneious (v.2021.1.1) using FastTree 2.1.11 and edited in FigTree v1.4.4 (http://tree.bio.ed.ac.uk/software/figtree/) and Adobe Illustrator version 25.4.1 (Adobe, San Jose, CA).

RESULTS

The raw transcriptome assembly resulted in 641,971 possible isoforms and 386,170 genes. The longest open reading frames (ORFs) were predicted and translated resulting in a set of 56,631 predictively complete protein sequences and an additional 31,671 partial sequences (including 5’ ends, 3’ ends and internal sequences). Further mapping and counting of raw reads to the assembled transcriptome allowed for identification of transcripts with very low counts that could be spurious (but no filtering was taken at this step to prevent loss of biologically relevant information).

D. depressana CYPome

An initial keyword search for P450s into the functional annotations in the raw transcriptome generated a list of 1,143 candidates. The list was further filtered by identifying the corresponding translated sequencing, narrowing down to 776 sequences. With respect to these 776 putative P450s, reciprocal BLAST search of candidate P450s against 7 other Lepidoptera species with complete/clean annotated CYPomes narrowed down the list to 61 P450s. Because it is expected that there are P450s in *D. depressana* that are not necessarily orthologs with other Lepidoptera P450s, additional BLAST searches into the transcriptome added 19 other sequences. A final list of 79 candidates was sent to Dr. David R. Nelson for official naming and to confirm orthologs. Ultimately, 76 P450 genes were named, including 15 unique sequences without close orthologues in related taxa. The *D. depressana* CYPome comprises 7 Clan 2, 37 Clan 3, 24 Clan 4, and 11 mitochondrial clan P450s (Table 3.1).

Differential expression analysis

Cross treatment analysis revealed 2,012 transcripts differentially expressed by two-fold or more between xanthotoxin and unamended diet and 2,032 transcripts in the xanthotoxin-sphondin treatment comparison (FDR corrected p-value <0.05) (Fig. 3.1). However, only 3 transcripts were upregulated in the sphondin-unamended diet treatment comparison. Upon closer inspection, these transcripts were partial sequences that could not be functionally annotated.

Gene Ontology Clusters

The Gene Ontology (GO) enrichment analysis revealed that, within the differentially expressed genes in the xanthotoxin-unamended diet comparison, the most highly upregulated

tend to correspond to biological functions pertaining to DNA replication (GO:0004386, GO:0003887, GO:0006260), RNA transcription (GO:0003968, GO:0034062, GO:0097747, GO:0032197, GO:0003723), and metabolism (GO:0042402, GO:0016491) (Table 3.2). Those downregulated by xanthotoxin in comparison to unamended diet appear to be involved in the Golgi body apparatus (GO:0006892, GO:0048193, GO:0005794), ribosomal activity (GO:0005840, GO:0030686, GO:0030490), and MAPK cascade regulation (GO:0043409, GO:0043408) (Table 3.2). Similarly, the GO enrichment analysis performed on the xanthotoxin-sphondin comparison indicate that helicase activity (GO:0004386, GO:0003724), polymerase activity (GO:0004197, GO:0003887, GO:0004190, GO:0070001, GO:0034062, GO:0097747), and metabolic functions (GO:0044255, GO:0036094, GO:0019752, GO:0006629, GO:0019438, GO:0044281, GO:0016788, GO:0071704, GO:0043436) are key biological differences underlying genetic upregulation in response to xanthotoxin consumption relative to sphondin consumption (Table 3.3). Conversely, downregulated genes tended to correspond to protein localization (GO:0045184, GO:0033036, GO:0008104, GO:0034613, GO:0070727) and transport functions (GO:0015031, GO:0071705, GO:0015833, GO:0006313) when *D. depressana* larvae consumed xanthotoxin-containing diet relative to sphondin-containing diet (Table 3.3). Due to the lack of significant differential gene expression between the unamended control diet and sphondin treatments, no GO analysis was performed on this cross-treatment comparison.

P450 Phylogeny

The phylogenetic tree of P450s for all 8 species of Lepidoptera is presented in Figure 3.1. In total, 558 P450 protein sequences were aligned. The resulting tree comprises 1,115 nodes with ML support values ranging from 0.19 to 1.

DISCUSSION

My goal in this project was to describe the transcriptional landscape underlying furanocoumarin metabolism in *D. depressana* to characterize its detoxification capacity in the early stages of its colonization of North America. The *D. depressana* transcriptome also offers a unique opportunity to elucidate key differences between closely related species that have evolutionarily diverged in hostplant feeding specificity. I found dramatic upregulation across a wide variety of genes in response to dietary xanthotoxin in *D. depressana*, consistent with its status as a family-level specialist, as it may have fewer genes encoding enzymes specific to furanocoumarin substrates relative to the superspecialist *D. radiella* (Calla et al. 2017), which consumes hostplant tissues containing high amounts of multiple furanocoumarins. As such, *D. depressana* may rely more heavily on more "promiscuous", or less substrate-specific, enzymes that perform more generalized functions during the detoxification of xenobiotics (Cheng et al. 2011; Gup et al. 2016). That oligophagous herbivores have more specialized detoxification enzymes than do more generalized consumers is a hypothesis that has been directly tested via examination of the CYPome of Lepidoptera across multiple taxa representing a broad spectrum of feeding strategies (Calla et al. 2017). Indeed, Calla et al. (2017) found that CYPome size is a direct function of Clan 3 size. However, unlike the treatment effect of dietary xanthotoxin, experimental diets containing 0.02% sphondin did not appear to induce significant differential

expression in the *D. depressana* transcriptome. While it cannot be discounted that the dearth of hostplants producing high amounts and structural variants of angular furanocoumarins in the diet of *D. depressana* (Chapter 1) may explain the apparent lack of differential regulation within the transcriptome, it seems unlikely that no other genes involved in stress response would be upregulated. Thus, these results are likely due to experimental idiosyncrasies, perhaps caused by differential exposure to or consumption of *D. depressana* to sphondin in the diet.

Gene Ontology terms grouping sets of the most highly expressed genes show many striking patterns of over-representation in response to xanthotoxin consumption, particularly with respect to transcription and translation processes. These processes are likely fundamental to meeting the physiological demands of increased metabolic activity and cellular damage repair. In terms of xenobiotic metabolism, the cytochrome complex (GO:0070069), mitochondrial transmembrane transport (GO:1990542), and oxioreductase activity (GO:0016491) GO terms recovered in the xanthotoxin-unamended diet comparison are all suggestive of increased cytochrome P450-mediated detoxification (Lyanagi et al. 2012). Similarly, GO terms recovered in the xanthotoxin-sphondin comparison such as organic substance metabolic process (GO:0071704) likely also facilitate P450 activity. These patterns of widespread differential expression are consistent with the hypothesis that a more generalized response to dietary furanocoumarins is employed by more generalized feeders due to relaxed selective pressure relative to super-specialists.

CYPome comparisons between *D. depressana* and *D. radiella* reveal close similarity in terms of gene number and categorical proportions. Both species have 7 Clan 2 genes, while *D. radiella* has 3 more Clan 3 genes than *D. depressana* (37 and 34, respectively), 1 more Clan 4 gene (24 and 23, respectively), and 1 fewer mitochondrial clan P450 (11 and 12, respectively)

(Calla et al. 2017) (Table 3.4). Clan 3 P450s are generally associated with detoxification of xenobiotics and Clan 4 P450s serve a variety of functions, including detoxification (Feyereisen 2012, 2020). The increase in Clan 3 and Clan 4 P450s in *D. radiella* supports the hypothesis that a more specialized herbivore requires a greater diversity of specialized enzymes to cope with the increased metabolic load associated with the greater consumption of toxic phytochemicals. One of the Clan 3 genes that is present in the *D. radiella* CYPome and absent in the *D. depressana* CYPome is CYP6AB3, which has been implicated in the detoxification of imperatorin (Mao et al. 2006). Imperatorin is present in *P. sativa*, a primary hostplant of *D. depressana* in late spring before *D. carota* is seasonally available in central Illinois. The CYP6 subfamily is widely implicated in the detoxification of furanocoumarins, and *D. depressana* appears to have as many genes in this family as *D. radiella*, albeit in different proportions. *Depressaria depressana* possesses one fewer CYP6AN gene, 1 more CYP6AW gene, and no CYP6CT genes. *Depressaria depressana* also appears to possess two pseudogenes, 1 in Clan 3 (CYP321C22-p) and 1 in Clan 4 (CYP4M90-p). Of the 15 genes with no known orthologues in closely related species, 8 are in Clan 3, 5 are in Clan 4, and 2 are in the Mitochondrial Clan. The unique CYP genes in Clan 3 may be involved in the detoxification of phytochemicals that *D. radiella* does not encounter in its two host genera. *D. depressana* possesses fewer CYP genes than any of the other species of Lepidoptera incorporated into the phylogeny, which includes *B. mori* (80), *P. xylostella* (85), *C. suppressalis* (78), *M. sexta* (103), *A. transitella* (89), and *O. brumata* (102). However, it does possess as many as or more Clan 3 CYP genes than the genus- or family-level specialists.

The CYPome phylogeny illustrates that, for the most part, subfamily relationships across taxa were retained, and orthologues between *D. radiella* and *D. depressana* were almost always

in the same clade as sisters. However, relationships involving novel CYP genes were uncovered in the P450 tree. As an example, CYP6AE1, a gene associated with detoxification of angular furanocoumarins in *D. radiella*, is nearly identical (98.357%) in both *Depressaria* species and was not upregulated in *D. depressana* as a result of consuming sphondin. However, sister to the CYPAE1 genes in these two species is CYP6AE126, which is unique to *D. depressana*. Future targeted gene expression studies could investigate the regulation of this gene in response to other phytochemicals that may be present in the diet of *D. depressana*. Another example is CYP6B227 in *D. depressana*, which is sister to the group comprising CYP6B66 and CYP6B67. The CYP6B family displays varying degrees of specificity across Lepidoptera, and CYP6B1 has been implicated in the metabolism of linear furanocoumarins in *P. polyxenes* (Li et al. 2004), whereas CYP6B66 was highly expressed in both linear and angular furanocoumarin treatments in *D. radiella* (Calla et al. 2017). As such, CYP6B227 is a potential candidate for furanocoumarin detoxification in *D. depressana*. Also worthy of note is that Calla et al. (2017) found no evidence of duplication of CYP6AW1 in the phylogeny, which apparently was lost in *P. xylostella*. Here, I found that CYP6AW2 appears to have arisen from CYP6AW1 via a duplication event and is present in *D. depressana*. A similar duplication event appears to have given rise to several Clan 4 genes, including CYP4S47, which is sister to CYP4S46 in both species of *Depressaria*. Entirely new Clan 4 genes, possibly resulting from a neofunctionalization event, are also observed in the form of CYP341A46 and CYP341A47, which are most closely related to CYP341A24 in *D. radiella*, and CYP367A22, which is sister to the clade containing CYP367A1 in both species of *Depressaria*.

The present study shows that, whereas *D. depressana* is well adapted to consume plant material containing large amounts of certain furanocoumarins, notably xanthotoxin in the

reproductive tissues of *P. sativa*, doing so requires a dramatic transcriptomic response, especially when compared to *D. radiella* (Calla et al. 2017). This pattern suggests that a relatively broader host range is enough to relax selection for specialization of detoxifying P450s. Moreover, while the reduced transcriptomic response to dietary sphondin observed in this investigation may have been exacerbated to experimental conditions, *D. depressana* may nevertheless be poorly suited to adopt native hosts producing high amounts of angular furanocoumarins, such as *H. maximum*. Taken together, these results demonstrate the need for current ecological studies that not only investigate differences between contrasting feeding strategies relative to diet breadth, but also consider the entirety of the feeding continuum and consider differences underlying narrower adaptive divergences among closely related species.

TABLES AND FIGURE

Table 3.1 The *Depressaria depressana* CYPome subdivided by clan.

CYP2 Clan	CYP3 Clan	CYP4 Clan	Mitochondrial Clan
CYP15C1	CYP6B66	CYP4G135	CYP301A1
CYP18A1	CYP6B67	CYP4G136	CYP301B1
CYP303A1	CYP6B227	CYP4G137	CYP302A1
CYP304F1	CYP6AB102	CYP4L35	CYP302A3
CYP305B1	CYP6AB103	CYP4L36	CYP315A1
CYP306A4	CYP6AB202	CYP4M52	CYP333A15
CYP307A2	CYP6AE1	CYP4M55	CYP333A29
	CYP6AE89	CYP4M56	CYP333B36
	CYP6AE90	CYP4M90-p	CYP333B37
	CYP6AE91	CYP4S27	CYP333B38
	CYP6AE92	CYP4S46	CYP339A1
	CYP6AE96	CYP4AU1	CYP428A1
	CYP6AE126	CYP4AU2	
	CYP6AE175	CYP340Q6	
	CYP6AE176	CYP340Q7	
	CYP6AN25	CYP341A46	
	CYP6AN27	CYP341A47	
	CYP6AN53	CYP341B25	
	CYP6AW1	CYP341B30	
	CYP6AW2	CYP367A1	
	CYP6JV1	CYP367A22	
	CYP9A7	CYP367B1	
	CYP9A94	CYP405A9	
	CYP9A96		

Table 3.1 (cont.)

CYP9A96
CYP9G33
CYP321C9
CYP321C22-p
CYP324A21
CYP324A46
CYP332A13
CYP332A49
CYP338A1
CYP354A18
CYP365A1

Table 3.2 Xanthotoxin vs. control diet differentially regulated genes GO term enrichment.

Top 20 Upregulated Genes GO Term Enrichment		
Gene	**Term**	**P Value**
GO:0004386	Helicase Activity	0.000372772
GO:0003724	RNA Helicase Activity	0.000974828
GO:0003887	A Polymerase Activity	0.001705374
GO:1901362	Organic Cyclic Compound Biosynthetic Process	0.001757153
GO:0004197	Cysteine-type Endopeptidase Activity	0.00201934
GO:0019438	Aromatic Compound Biosynthetic Process	0.00308256
GO:0003968	RNA-Directed 5'-3' RNA Polymerase Activity	0.003468586
GO:0034062	5'-3' RNA Polymerase Activity	0.003468586
GO:0097747	RNA Polymerase Activity	0.003468586
GO:0070925	Organelle Assembly	0.004502047
GO:0018130	Heterocycle Biosynthetic Process	0.005466811
GO:0006260	DNA Replication	0.006787363
GO:0032197	Transposition, RNA-Mediated	0.00752618
GO:0003723	RNA Binding	0.008542982
GO:0009310	Amine Catabolic	0.011960172
GO:0042402	Cellular Biogenic Amine Catabolic Process	0.011960172
GO:0070069	Cytochrome Complex	0.013679645
GO:1990542	Mitochondrial Transmembrane Transport	0.014048596
GO:0008234	Cysteine-Type Peptidase Activity	0.015099178
GO:0016491	Oxidoreductase Activity	0.015151758
Top 20 Downregulated Genes GO Term Enrichment		
Gene	**Term**	**P Value**
GO:0005840	Ribosome	0.002437243

Table 3.2 (cont.)

GO:0030312	External Encapsulating Structure	0.002614404
GO:0005618	Cell Wall	0.004592652
GO:0043409	Negative Regulation of MAPK Cascade	0.010704289
GO:0034613	Cellular Protein Localization	0.011233985
GO:0044272	Sulfur Compound Biosynthetic Process	0.011233985
GO:0046434	Organophosphate Catabolic Process	0.015820458
GO:0048193	Golgi Vesicle Transport	0.01843692
GO:0005794	Golgi Apparatus	0.018635442
GO:0006914	Autophagy	0.020316598
GO:0034097	Response to Cytokine	0.020516973
GO:0070727	Cellular Macromolecule Localization	0.021968493
GO:0006892	Post-Golgi Vesicle-Mediated Transport	0.022012865
GO:0044389	Ubiquitin-Like Protein Ligase Binding	0.023442411
GO:0051020	GTPase Binding	0.02375143
GO:0071705	Nitrogen Compound Transport	0.025240964
GO:0043408	Regulation of MAPK Cascade	0.027748221
GO:0030490	Maturation of SSU-rRNA	0.027748221
GO:0030686	90S Preribosome	0.028159414
GO:0000139	Cellular Response to Cytokine Stimulus	0.028159414

Table 3.3 Xanthotoxin vs. sphondin differentially regulated genes GO term enrichment.

Top 20 Upregulated Genes GO Term Enrichment		
Gene	**Term**	**P Value**
GO:0004386	Helicase Activity	5.10E-05
GO:0003824	Catalytic Activity	0.000336344
GO:0003968	RNA-Directed 5'-3' RNA Polymerase Activity	0.000670765
GO:0004197	Cysteine-Type Endopeptidase Activity	0.000908012
GO:0003887	DNA-Directed DNA Polymerase Activity	0.00110134
GO:0003724	RNA Helicase Activity	0.001597415
GO:0004190	Aspartic-Type Endopeptidase Activity	0.00159893
GO:0070001	Aspartic-Type Peptidase Activity	0.00159893
GO:0034062	5'-3' RNA Polymerase Activity	0.002207027
GO:0097747	RNA Polymerase Activity	0.002207027
GO:0044255	Cellular Lipid Metabolic Process	0.003100776
GO:0036094	Small Molecule Binding	0.004004287
GO:0019752	Carboxylic acid Metabolic Process	0.004363994
GO:0006629	Lipid Metabolic Process	0.004665628
GO:0019438	Aromatic Compound Biosynthetic Process	0.004954003
GO:0044281	Small Molecule Metabolic Process	0.005307143
GO:0016788	Hydrolase Activity, Acting on Ester Bonds	0.005514826
GO:0071704	Organic Substance Metabolic Process	0.006074313
GO:0043436	Oxoacid Metabolic Process	0.006751417
GO:0006082	Organic Cyclic Compound Biosynthetic Process	0.006813584
Top 20 Downregulated Genes GO Term Enrichment		
Gene	**Term**	**P Value**
GO:0032989	Cellular Component Morphogenesis	0.002478593

Table 3.3 (cont.)

GO:0015031	Protein Transport	0.002908068
GO:0045184	Establishment of Protein Localization	0.004610179
GO:0030490	Maturation of SSU-rRNA	0.005177497
GO:0030686	90S Preribosome	0.005177497
GO:0042886	Amide Transport	0.0052576
GO:0033036	Macromolecule Localization	0.005302161
GO:0071705	Nitrogen Compound Transport	0.005548972
GO:0008104	Protein Localization	0.005631168
GO:0015833	Peptide Transport	0.005761844
GO:0016197	Endosomal Transport	0.005948547
GO:0048193	Golgi Vesicle Transport	0.007467549
GO:0032990	Cell Part Morphogenesis	0.00778887
GO:0034613	Cellular Protein Localization	0.011761155
GO:0048812	Neuron Projection Morphogenesis	0.012542824
GO:0048858	Cell Projection Morphogenesis	0.012542824
GO:0070727	Cellular Macromolecule Localization	0.012786795
GO:0070271	Transposition, DNA-Mediated	0.012863459
GO:0006313	Intracellular Protein Transport	0.017278611
GO:0006886	Ribosome	0.017312646

Table 3.4 Comparison of lepidopteran CYPomes from Calla et al. (2017) and newly generated *Depressaria depressana* CYPome presented in this study.

	Clan 2	Clan 3	Clan 4	Mit.	Total	Feeding
Depressaria radiella	7	37	24	11	79	Species specialist
Depressaria depressana	7	34	23	12	76	Family specialist
Chilo suppressalis	7	34	28	11	78	Polyphagous
Bombyx mori	7	32	30	11	80	Species specialist
Amyelois transitella	8	41	41	11	89	Polyphagous
Plutella xylostella	10	26	35	14	85	Family specialist
Operophtera brumata	10	32	42	12	102	Polyphagous
Manduca sexta	8	45	34	16	103	Family specialist

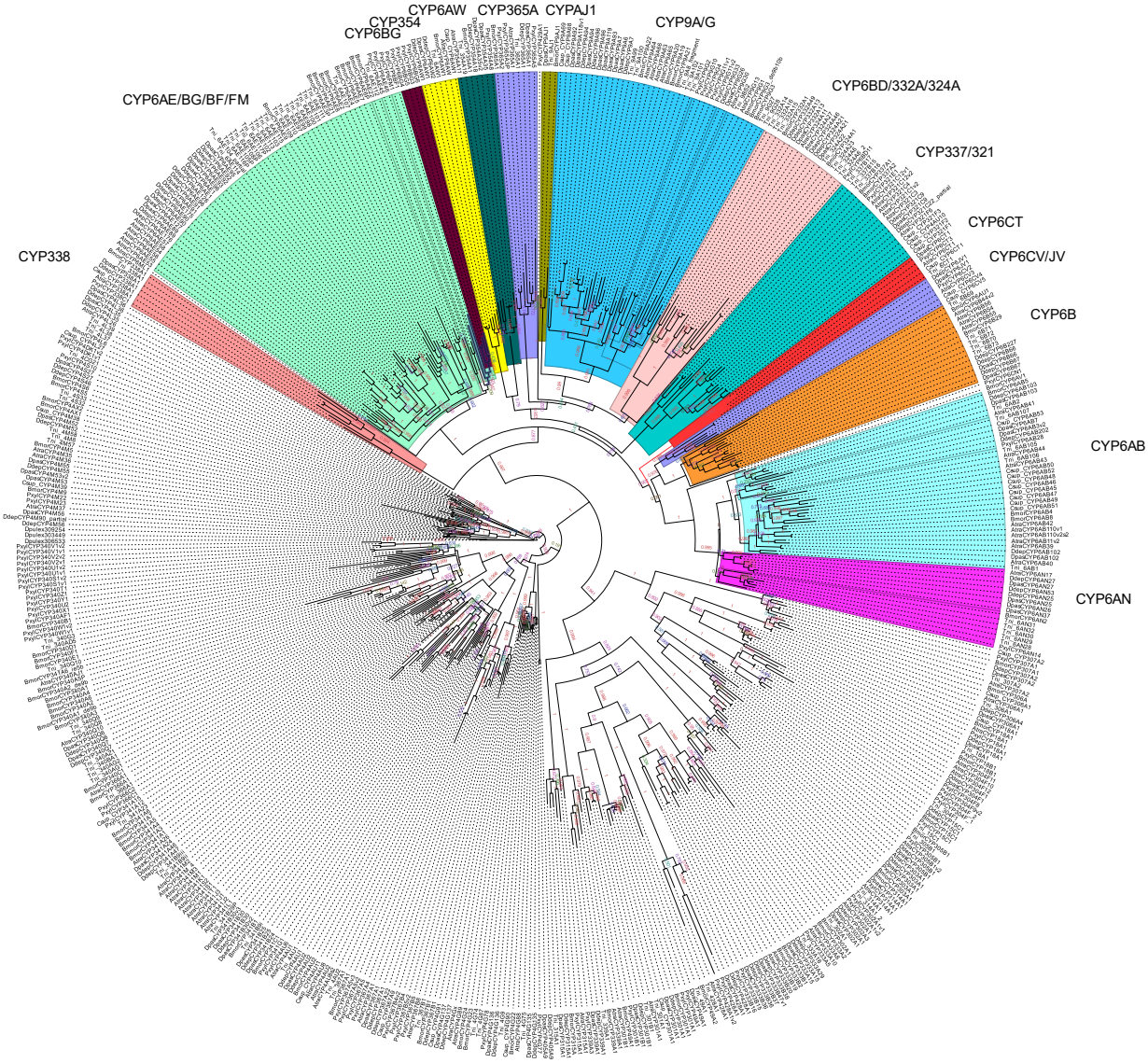

Figure 3.1 Rooted cytochrome P450 phylogeny with Clan 3 P450s highlighted. The species represented in this phylogeny are *Daphnia pulex*, *Depressaria depressana*, *Depressaria radiella*, *Chilo suppressalis*, *Amyelois transitella*, *Trichoplusia ni*, *Bombyx mori*, and *Plutella. xylostella*. Branch labels represent ML support values.

REFERENCES

Berenbaum MR (1983) Coumarins and caterpillars: a case for coevolution. Evolution 37: 163-179.

Berenbaum MR (1991) Coumarins. In: Rosenthal G, Berenbaum MR (ed) Herbivores their interactions with secondary plant metabolites. NY: Academic Press pp 221-249.

Berenbaum MR, Zangerl AR (1991) Acquisition of a native hostplant by an introduced oligophagous herbivore. Oikos 62:153-159.

Berenbaum MR, Zangerl AR (1996). Phytochemical diversity: adaptation or random variation?. in Phytochemical Diversity and Redundancy in Ecological Interactions (J. Romeo et al., eds) (pp. 1-24). Springer US.

Berenbaum MR, Zangerl AR, Nitao JK (1986) Constraints on chemical coevolution; wild parsnips and the parsnip webworm. Evolution 40: 1215-1228.

Bolger AM, Lohse M, Usadel B (2014). Trimmomatic: A flexible trimmer for Illumina sequence data. Bioinform 30: 2114 -2120.

Bryant DM, Johnson K, DiTommaso T, Tickle T, Couger MB, Payzin-Dogru D, Lee TJ, Leigh ND, Kuo TH, Davis FG, Bateman J, Bryant S, Guzikowski AR, Tsai SL, Coyne S, Ye WW, Freeman RM Jr, Peshkin L, Tabin CJ, Regev A, Haas BJ, Whited JL (2017) A tissue-mapped axolotl de novo transcriptome enables identification of limb regeneration factors. Cell Rep 18: 762-776.

Calla B (2021) Signatures of selection and evolutionary relevance of cytochrome P450s in plant-insect interactions. Curr Opin Insect Sci 43: 92-96.

Calla B, Hall B, Hou S, Geib SM (2014) A genomic perspective to assessing quality of mass-reared SIT flies used in Mediterranean fruit fly (*Ceratitis capitata*) eradication in California. BMC Genom 15.

Calla B, Noble K, Johnson RM, Walden KKO, Schuler MA, Robertson HM, and Berenbaum MR (2017) Cytochrome P450 diversification and hostplant utilization patterns in specialist and generalist moths: Birth, death and adaptation. Mol Ecol 26: 6021–6035.

Calla B, Wu WY, Dean CAE, Schuler MA, Berenbaum MR (2020). Substrate-specificity of cytochrome P450-mediated detoxification as an evolutionary strategy for specialization on furanocoumarin-containing hostplants: CYP6AE89 in parsnip webworms. Insect Mol Biol 29: 112–123.

Feyereisen R (2006) Evolution of insect P450. Biochem Soc Trans 34: 1252-1255.

Feyereisen (2012) Insect CYP genes and P450 enzymes. Insect Mol Biol Biochem 450: 236-316.

Haas BJ, Papanicolaou A, Yassour M, Grabherr M, Blood PD, Bowden J, Couger MB, Eccles D, Li B, Lieber M, Macmanes MD, Ott M, Orvis J, Pochet N, Strozzi F, Weeks N, Westerman R, William T, Dewey CN, … Regev A (2013) De novo transcript sequence reconstruction from RNA-seq using the Trinity platform for reference generation and analysis. Nat Protoc 8: 1494–1512.

Harrison T, Dean CAE, Parks K, Berenbaum MR (2016) *Depressaria depressana* (fabricius) (depressariidae), new to the Midwestern USA. J Lepid Soc 70: 169–173.

Hoi KK, Daborn PJ, Battlay P, Robin C, Batterham P, O'Hair RA, Donald WA (2014) Dissecting the insect metabolic machinery using twin ion mass spectrometry: a single P450 enzyme metabolizing the insecticide imidacloprid in vivo. Anal Chem 86: 3525-3532.

Iga M, Kataoka H (2012) Recent studies on insect hormone metabolic pathways mediated by cytochrome P450 enzymes. Biol Pharm Bull 35: 838-843.

Jackson CJ, Liu JW, Carr PD, Younus F, Coppin C, Meirelles T, Lethier M, Pandey G, Ollis DL, Russell RJ, Weik M (2013) Structure and function of an insect α-carboxylesterase (αEsterase7) associated with insecticide resistance. PNAS 110: 10177-10182.

Li B, Dewey CN (2011) RSEM: accurate transcript quantification from RNA-Seq data with or without a reference genome. BMC Bioinform 12: 1-6.

Mao W, Rupasinghe S, Zangerl AR, Schuler MA, Berenbaum MR (2006) Remarkable substrate-specificity of CYP6AB3 in *Depressaria pastinacella*, a highly specialized caterpillar. Insect Mol Biol 15: 169-179.

Merzendorfer H (2014) ABC transporters and their role in protecting insects from pesticides and their metabolites. Adv In Insect Phys 46: 1-72.

Nauen R, Zimmer CT, Vontas J (2021) Heterologous expression of insect P450 enzymes that metabolize xenobiotics Curr Opin Insect Sci 43: 78-84.

Neve EP, Eliasson E, Pronzato MA, Albano E, Marinari U, Ingelman-Sundberg M (1996) Enzyme-specific transport of rat liver cytochrome P450 to the Golgi apparatus. Arch Biochem Biophys 333: 459-65.

Nitao JK, Berenbaum MR (1988) Laboratory Rearing of the Parsnip Webworm, *Depressaria pastinacella* (Lepidoptera: Oecophoridae). Ann Entomol Soc Am 81: 485-487.

Nitao JK, Berhow M, Duval SM, Weisleder D, Vaughn SF, Zangerl A, Berenbaum MR (2003) Characterization of furanocoumarin metabolites in parsnip webworm, *Depressaria pastinacella*. J Chem Ecol 29: 671-682.

Pavlidi N, Vontas J, Van Leeuwen T. The role of glutathione S-transferases (GSTs) in insecticide resistance in crop pests and disease vectors (2018) Curr Opin Insect Sci 27: 97-102.

Robinson MD, McCarthy DJ, Smyth GK (2010) EdgeR: a Bioconductor package for differential expression analysis of digital gene expression data. Bioinform 26: 139-140.

Schuler MA (2011) P450s in plant–insect interactions. Biochim Biophys Acta Proteins Proteom 1814: 36-45.

Scott JG, Wen Z (2001) Cytochromes P450 of insects: the tip of the iceberg. Pest Manag Sci 57: 958-967.

Sezutsu H, Le Goff G, Feyereisen R (2013) Origins of P450 diversity. Philos Trans R Soc Lond B Biol Sci 368: 20120428.

Simon JY (1996) Insect glutathione S-transferases. Zool Stud 35: 9-19.

Wen Z, Rupasinghe S, Niu G, Berenbaum MR, Schuler MA (2006) CYP6B1 and CYP6B3 of the black swallowtail (*Papilio polyxenes*): adaptive evolution through subfunctionalization. Mol Biol Evol 23: 2434-2443.

Wu C, Chakrabarty S, Jin M, Liu K, Xiao Y (2019) Insect ATP-binding cassette (ABC) transporters: roles in xenobiotic detoxification and Bt insecticidal activity. Int J Mol Sci 20: 2829.

Zangerl AR, Berenbaum MR (2003) Phenotype matching in wild parsnip and parsnip webworms: causes and consequences. Evol 57: 806-815.

CHAPTER 4

WESTWARD EXPANSION OF *DEPRESSARIA DEPRESSANA* (LEPIDOPTERA: DEPRESSARIIDAE): POPULATION GENETIC STRUCTURE AND DISPERSAL ROUTE

INTRODUCTION

A major rise in the number of invasive species in North America has occurred over the past 50 years as a direct result of increased globalization (Pysek and Richardson 2010; Mack et al. 2000; Palumbi 2001). Managing the introduction of exotic insect species into new habitats is particularly problematic owing to their typical ease of transport, adaptability to new environments, rapid generation times, and high reproductive capacity (Peacock and Worner 2008; McLaughlin and Dearden 2019). In North America alone, there are more than 470 introduced insect species (Center for Invasive Species and Ecosystem Health, invasive.org), which annually incur costs exceeding $23 billion in the region (Bradshaw et al. 2016). This damage includes substantial loss of native biodiversity, loss of ecosystem services, crop yield loss, destruction of infrastructure, and declines in human health. Developing successful prevention and management practices is predicated upon a thorough understanding of both the ecological and evolutionary processes underlying insect colonization of novel habitats. To that end, monitoring the spread of a recently introduced species offers a unique opportunity to develop models of insect dispersal across, and adaptation to, new environments.

The purple carrot-seed moth *Depressaria depressana* (Lepidoptera: Depressariidae), native to Eurasia, was first documented in the scientific literature as an introduced species in the United States in 2015 (Harrison et al. 2016) and has likely been established in North America

since at least 2008 (Landry et al. 2013), with images of larvae and adults appearing on BugGuide from New York, Connecticut, and Massachusetts as early as 2010. Although restricted to hostplants in the family Apiaceae, *D. depressana* utilizes species across a wide taxonomic cross-section of the family (Harrison et al. 2016). Moreover, in contrast with most *Depressaria* species, it is multivoltine and exhibits seasonal activity from late spring to early fall in central Illinois (personal observation).

In expanding its range to include North America, *D. depressana* follows its Eurasian congener *D. radiella* (formerly *D. pastinacella*), which was first reported in the Western Hemisphere in Ontario in 1862 (Bethune 1869, named *Depressaria ontariella* and subsequently synonymized with the European *D. heracliana*). Like *D. depressana*, *D. radiella* is associated with hostplants in the family Apiaceae but it is essentially restricted to two genera in the closely related genera *Heracleum* and *Pastinaca* and throughout its range is univoltine. Early reports of its occurrence in North America were associated with the damage it inflicted on flowers and fruits of *Pastinaca sativa*, the edible parsnip (Bethune 1869, Riley 1889, Southwick 1892, Busck 1902, Brittain and Gooderham 1916). *P. sativa* is an apiaceous weedy biennial native to Eurasia that has been domesticated as a root vegetable. Both wild and domesticated forms were introduced to North America in the seventeenth century (Averill and DiTommaso 2007) and the range of the interaction between parsnip webworms and the wild parsnip now extends across much of Canada and the United States (Averill and DiTommaso 2007).

Examination of *P. sativa* sampled from herbarium collections revealed that North American wild parsnip populations increased in toxic furanocoumarin content shortly after the accidental introduction of *D. radiella* to North America (Zangerl and Berenbaum 2005) and that, within its midwestern US range, parsnip webworms exhibit population-level detoxification

profiles reflecting the furanocoumarin profiles in the immature fruits of their corresponding hostplant populations (Berenbaum and Zangerl 1992). The reestablishment of the *D. radiella* and *P. sativa* system across novel landscapes has since been repeated in New Zealand. In 2004, *D. radiella* was first documented in Dunedin roughly 150 years after the introduction of *P. sativa* (Patrick 2004). Studies conducted over a six-year period after the introduction of *D. radiella* to New Zealand found that *P. sativa* fitness was adversely affected following a reduction in seed production by up to 75% in six previously uninfested populations. As a compensatory mechanism, *P. sativa* populations in New Zealand, which were distinct from European and North American populations in phytochemical profile, exhibited increased growth rate accompanied by greater production of the floral volatile octyl butyrate (Zangerl et al. 2008).

For more than 40 years, the relationship between wild parsnip and the parsnip webworm *D. radiella* has served as a useful model for studying exotic plant-insect reassociations within and across novel landscapes (Agrawal and Zhang 2021). While the colonization of *D. radiella* across multiple continents provides an exemplar of rapid ecological and evolutionary change following establishment of an invasive species, it is inherently constrained by the tightly coevolved nature of the *D. radiella-P. sativa* relationship. Since its introduction more than 140 years ago, for example, *D. radiella* has acquired only a single native hostplant, *Heracleum maximum*, American cow-parsnip, the sole North American congener of many of its European hostplants (Berenbaum and Zangerl 1991). *D. depressana*, however, utilizes a broader array of host plants in its native range species and has been associated with at least a dozen additional apiaceous genera in a diversity of tribes across Eurasia (Chapter 1). Moreover, the extended period of seasonal activity of *D. depressana*, combined with its status as a family-level specialist, suggests that, while the selection pressure exerted on its many hostplants may be less intense

than that exerted by its congener, the broader host range and extended period of seasonal activity suggest that this species has a greater likelihood of encountering and acquiring native North American plants as novel hosts (Chapter 1). Investigating the colonization of family-specialist *D. depressana* across North America can serve as a unique comparative measure against that of the "superspecialist" *D. radiella* (restricted to only two genera) and may inform predictions of the potential selective impact of invasive herbivores as a function of diet breadth.

A critical component of tracking ongoing biological invasions is the assessment of populational genetic structure along putative routes of establishment, which can facilitate inferences as to the source population, mode of introduction, and rate of evolution. In this study, I employed the use of two molecular markers, mitochondrial cytochrome c oxidase subunit I (COI) and nuclear elongation factor 1-alpha (EF1α), to assess the population genetic structure of *D. depressana* in the eastern United States. As a nuclear gene, EF1α is not exclusively maternally inherited, so its inclusion alongside COI allows gene flow to be assessed in a more balanced way. Using these markers, I constructed haplotype networks to evaluate the inter- and intra-populational genetic diversity across both latitudinal and longitudinal gradients to the north and east of Illinois, where *D. depressana* was first reported in the United States (Harrison et al. 2016). I also constructed a haplotype network incorporating both European and North American *D. radiella*, using COI barcodes available in the BOLD (Ratnasingham and Hebert 2007) database. Lastly, using historical publications and museum records, I reconstructed an approximate timeline of the range expansion of *D. radiella* across North America. Together, the COI haplotype network and the approximate invasion timeline of the superspecialist *D. radiella* will provide a comparative insight as to whether the ecological differences in diet breadth and period of seasonal activity influence population structure across geographic space and whether

this will ultimately influence the rate of successful *D. depressana* establishment across North America.

METHODS

D. depressana sampling

D. depressana larvae were sampled from the umbels of wild carrot *Daucus carota* at eight different collection sites along a latitudinal gradient from Urbana, IL to Eau Claire, WI in July 2020 and nine collection sites along a longitudinal axis from Urbana, IL to Newburg, PA in July 2021. Ten ultimate instar larvae were collected from each site and preserved in labeled glass tubes filled with 90% EtOH. The state and GPS coordinates corresponding to each collection site are given in Table 4.1. These GPS locations presented in maps in Figure 4.1.

DNA extractions PCR amplification

For freshly collected specimens, total genomic DNA was collected from whole-body tissue extractions of *D. depressana* using the Qiagen DNeasy Blood and Tissue Kit (Qiagen Inc., Valencia, California) following the manufacturer's protocol. Ultimate instar caterpillars were individually homogenized in a solution containing buffer ATL and proteinase K using an autoclavable pestle (Fisher Scientific, Hampton, NH). The homogenized tissue was incubated at 56ºC for 1 h to ensure complete cell lysis. A series of wash buffers was used to remove RNA, proteins, and other contaminants from the solution before DNA was ultimately eluted in 50 µl of ddH_2O. DNA concentration was assessed via Nanodrop spectrophotometer (Thermo Fisher Scientific, Waltham, Massachusetts).

PCR amplification was performed for ribosomal COI and nuclear EF1α. The partial sequence of COI was amplified with the following primers: (forward) 5' GGTCAACAAATCATAAAGATATTGG 3' and (reverse) 5' TAAACTTCAGGGTGACCAAAAAATCA 3' generating a 658 bp amplicon. The partial sequence of EF1α was amplified with the following primers: (forward) 5' GTCACCATCATYGACGC 3' and (reverse) 5' GATACCAGTCTCAACTCTTCC 3' generating a 517 bp amplicon. Onetaq polymerase was used for both PCR reactions (New England Biolabs, Ipswich, Massachusetts). PCR conditions were 95ºC/1 min for the initial denaturation phase, then 40 cycles of 95ºC/30 s, 50ºC/30 s, 68ºC/1 min, followed by a final extension phase at 72ºC/5 mins. Sanger sequencing was performed at the Keck Center at University of Illinois, Urbana-Champaign. Additionally, COI barcodes were sourced from the BOLD database (Ratnasingham and Hebert 2007) to be included in the COI haplotype network as a comparative measure to evaluate potential source populations. Similarly, COI barcodes for *D. radiella* were also obtained from BOLD for reconstruction of European and North American haplotypes.

Alignment and Gene Characterization

Raw sequence reads were imported to Geneious (2021.1.1) and ends were trimmed using an error probability limit of 0.05. Complementary paired sequences were assembled *de novo*, read quality was visually assessed by distinctness of fluorescence peaks, and heterozygotes were manually corrected. The consensus regions were then extracted, and primer regions were trimmed. All COI sequences were aligned in Geneious via the MAFFT version 7.450 alignment algorithm (Katoh and Standley 2008) using default parameters

Haplotype Network Construction and Analysis

Partial sequences for COI and EF1α were exported separately in Nexus file format. The Nexus files included trait blocks incorporating population assignments. Haplotype designations and networks were generated in PopART (Leigh and Bryant 2015) using the Templeton-Crandall-Sing (TCS) algorithm (Clement et al. 2000). Genetic variation across populations was assessed across geographic space via analysis of molecular variance (AMOVA).

Reconstruction of the Establishment of *D. radiella* Across the USA and Canada

Publications documenting the earliest observations of *D. radiella* in North American states and provinces were retrieved from PubMed.gov. Search terms "*Depressaria pastinacella*" "*Depressaria heracliana*" and "*Depressaria ontariella*" were used and the results were filtered by date. Additionally, physical copies of publications documenting early observations of *D. radiella* in North America were included in this analysis. These publications were retrieved from the private collection of Dr. May Berenbaum at University of Illinois. Searches for *D. radiella* museum records were performed in iDigBio.org using the query terms "*Depressaria radiella*" or "*Depressaria pastinacella*" with United States and Canada as the "Country" specification. Search results were filtered by "Date" and "State/Province" of specimen collection. The earliest museum record of every state or province was used in the analysis and the corresponding museum was noted.

RESULTS

I amplified and sequenced the COI locus for 167 *D. depressana* individuals and the EF1α locus for 153 individuals. Due to COVID-related problems, I was unable to obtain the original

DNA extracts corresponding to the *D. depressana* barcodes retrieved from the BOLD database, which prevented me from amplifying and sequencing the EF1α locus for those individuals. Subsequently, only 34 sequences of COI were retrieved from the BOLD database and added to the alignment containing COI sequences generated in-house in Geneious for this analysis.

Across the ~680-km latitudinal gradient ranging from Urbana, IL to Eau Claire, WI, 79 COI sequences were generated from *D. depressana* collected across eight geographic locations. COI sequences from the 34 additional taxa retrieved from the BOLD database were incorporated into the 681-bp nucleotide alignment. Uncorrected pairwise COI distances revealed genetic distances of 0-2%. Within this alignment, 22 polymorphisms were identified as informative for the delineation of haplotypes, and individuals were subsequently clustered into eight distinct haplotypes (Figure 4.2). While high levels of genetic diversity were detected across all taxa, the results of the AMOVA indicates that diversity varies with geography at the level of $p = 0.059$ (AMOVA, $\phi_{ST} = 0.095$, $p = 0.059$).

Analysis of the ~1078 km longitudinal gradient ranging from Urbana, IL to Newburg, PA incorporated 88 *D. depressana* collected from nine geographic locations. For these specimens, 88 COI sequences were generated and aligned to the 34 COI sequences retrieved from the BOLD database. Seven informative polymorphisms were identified, and taxa were clustered into six distinct haplotypes. Similarly, genetic diversity corresponds to geographic location at a significance level of $p = 0.068$ (AMOVA, $\phi_{ST} = 0.12$, $p = 0.068$) (Figure 4.3).

Analysis of the 658 bp region of COI for *D. radiella* incorporated 42 individuals. Of these individuals, 7 were collected in the United States, 16 in Canada, and 19 from Europe. The resulting haplotype networks revealed two distinct haplotypes, with 5 informative SNPs distinguishing them. All individuals fell into the H1 haplotype, with the single *D. radiella*

collected in Russia constituting the H2 haplotype. Results from the AMOVA were highly significant (AMOVA, ϕ_{ST} = 0.99, p= 0.01) (Figure 4.4).

Within the 513 nucleotide positions of the EF1α alignments, genetic distances range from 1% to 3%. However, high numbers of mutational steps between taxa were recovered at this locus, resulting in far greater haplotype diversity compared to COI. For the 78 samples collected latitudinally from eight populations, individuals were clustered into 28 haplotypes (Figure 4.5) and the 75 samples collected longitudinally from nine populations were clustered into 29 haplotypes (Figure 4.6). AMOVA results indicated interactions between genetic diversity and geographical location at values of p ranging from 0.063 to 0.065 for samples collected both latitudinally (AMOVA, ϕ_{ST} = 0.069, p= 0.063) and longitudinally (AMOVA, ϕ_{ST} = 0.062, p= 0.065).

The literature search results and museum records used in establishing the timeline of the westward expansion of *D. radiella* across North America are presented in Table 4.2. The earliest recording of *D. radiella* in North America occurred in Ontario in 1862 and the earliest recording of *D. radiella* in the United States occurred in 1888 in Pennsylvania. Records show that, by 1889, *D. radiella* was successfully established across most of the eastern United States. *Depressaria radiella* was first observed on the west coast of the continent in Oregon in 1914.

DISCUSSION

COI is a widely used marker for assessing haplotype diversity in invasive and migratory Lepidoptera (Balbi et al. 2020; Li et al. 2006; Nagoshi et al. 2015; Nagoshi et al. 2012; Lee et al. 2020). This gene evolves at a relatively slow rate in Lepidoptera and generally displays low intraspecific diversity (Brower 1994). COI sequencing offers a reliable method of evaluating

competing hypotheses regarding invasive populations and their introduction pathways into new geographic areas. Sampling both field-collected and museum specimens of *Helicoverpa armigera* across Argentina, Balbi et al. (2020) uncovered 5 COI haplotypes, along with 3 cytochrome b (Cytb) haplotypes, which provided preliminary evidence of multiple points of introduction into the region from neighboring Latin American countries. Similarly, Lee et al. (2020) proposed that, among populations of *Spodoptera frugiperda*, a species recently introduced to South Korea, the two distinct COI haplotypes present were suggestive of Brazil populations as the source of this invasion. This study was the first to monitor the genetic distribution of *S. frugiperda*, which, given its high capacity for migration and dispersal, makes it a candidate to become a major agricultural pest in South Korea (Lee et al. 2020). In my study, I found 8 COI haplotypes among the eight populations spanning the latitudinal gradient, and six haplotypes among the nine populations spanning the longitudinal gradient. Across all COI sequences, I found evidence suggesting that populations established in geographic regions within the United States have genetically differentiated. This pattern is consistent with either multiple introductions of *D. depressana* or a single introduction of a large population retaining a large amount of diversity of ancestrally polymorphic alleles. While the dataset sampled from the BOLD database was limited, 6 haplotypes were recovered from the 35 sequences originating in Europe and Canada. However, the populations sampled in the United States do not strictly coincide to specific European or Canadian populations, consistent with ongoing interpopulational outcrossing or a lack of sufficient evolutionary time for geography-specific COI haplotypes to establish. Multiple introductions may indeed provide an adaptive advantage to *D. depressana*, as it reduces the likelihood of bottleneck events.

In contrast, the COI haplotype network for *D. radiella* reveals almost no distinct population structure within North America and across Europe. All individuals included in this analysis comprise a single haplotype except for one individual collected in Russia. This Russian individual was placed into a separate haplotype on the basis of four informative SNPs. Future studies incorporating a large sampling of Russian *D. radiella* may reveal whether geographic barriers obstruct gene flow between western European and Russian populations using a redundancy analysis (RDA). Nevertheless, the apparent decrease in genetic diversity at COI may indicate a slower rate of molecular evolution in *D. radiella* compared to *D. depressana*. Multiple generations per year and a lengthier period of seasonal activity in *D. depressana* may be predicated upon its expanded host range, which comprises apiaceous hosts that have sequential yet overlapping blooming periods throughout the year. More generations per breeding season and greater potential exposure to selective pressure exerted by host phytochemistry may explain the increased rate of molecular evolution in *D. depressana*.

EF1α generally provides a high phylogenetic signal in the Lepidoptera (Caterino et al. 2000) and is also often used in haplotype networks in conjunction with COI, particularly in the delineation of cryptic species (Wang et al. 2020; Cheng et al. 2016; van Nieurkerken et al. 2012). Van Nieurkerken et al. (2012) found that only EF1α was able to distinguish between several cryptic species within the leaf-mining subgenus *Ectodemia* (Nepticulidae). However, in other taxa, such as the rice stem borer *Chilo suppressalis* (Crambidae), EF1α sequencing recovered only one haplotype among populations feeding on rice (*Oryza sativa*) and water oats (*Zozamoa latifolia*), and the mitochondrial genes COI and COII were more informative (Wang et al. 2020). I found 28 EF1α haplotypes among the eight populations across the latitudinal gradient and 29 haplotypes among the nine populations across the longitudinal gradient. The high number of

haplotypes across both sampling axes obscures any meaningful signal of relatedness to putative source populations and/or dispersal routes. If the number of EF1α haplotypes in this study is indeed indicative of a large degree of genetic diversity, either through rapid environmental adaptation, multiple introductions, or a highly diverse founding population, *D. depressana* may be well suited to overcome novel environmental barriers in areas of introduction (Facon et al. 2006).

More than a century after the parsnip webworm first appeared in North America, reconstructing its history of westward and southward expansion is challenging, but, because of its status as an economic pest of cultivated parsnip, its first appearance in an area previously free of the pest often merited collection and preservation in a museum or a report in a journal. A survey of the literature and museum records relating to the expanding geographic distribution of the parsnip webworm reveals that *D. radiella* successfully expanded its range from the East Coast to the West coast in at most 52? years, between 1862 to 1914. In 1925, *D. radiella* was reported to have been established Yuma County in Arizona, bordering Mexico, which represents considerable southward expansion of its range. By 1932, Dustan (1932) noted that this species was present in "all provinces" of Canada. Given that *P. sativa* was a more heavily planted crop in the early part of the *D. radiella* colonization of North America, it remains to be seen whether *D. depressana* will be able to expand its range at the same pace as *D. radiella*. However, by virtue of its increased period of seasonal activity and given the ubiquity of alternative hosts, particularly *D. carota,* along North American highways, *D. depressana* may indeed require less time to colonize the continent.

This study is unique in that *D. depressana* is still apparently in the early stages of its invasion, whereas many similar studies assess population structure long after invasive species

have established. Invasive insects with relatively broad host ranges often have profound impacts on ecosystem dynamics, not only through imposing additional selection pressure on their food plants, but also in terms of competitive displacement of native insects and introduction of new pathogens (Snyder and Evans 2006). Whereas *D. radiella*, a superspecialist herbivore, reestablished its tightly coevolved relationship with *P. sativa* in North America (Zangerl et al. 2008; Jogesh et al. 2013), thereafter adopting a single alternate native host in *H. maximum* (Berenbaum and Zangerl 1991) as far as is known, *D. depressana* offers a novel comparator for assessing the ecological impact of less specialized Lepidoptera. One avenue of exploration would be to monitor the impact of *D. depressana* on wild carrot, *D. carota*, a non-native but long-established umbellifer with low levels of furanocoumarin production (Chen et al. 2001; Khalil et al. 2018). Intense florivory by *D. depressana* may select for greater production of furanocoumarins, as *D. radiella* did in *P. sativa* within 20 years of its introduction to North America (Berenbaum and Zangerl 2005), potentially altering the community structure of native insects consuming *D. carota* and may similarly affect native umbellifers, such as golden alexanders, *Zizia aurea*, the seeds of which are consumed by this species in the laboratory (Chapter 1).

TABLES AND FIGURES

Table 4.1 Sampling locations and GPS information for all *D. depressana* sampled in this experiment.

Site	State	Latitude	Longitude	Collection Date
1	Illinois 1	40.12854	-88.1439	July, 2020
2	Illinois 2	40.62144	-89.4234	July, 2020
3	Illinois 3	40.87883	-90.0877	July, 2020
4	Iowa 1	41.63711	-90.5679	July, 2020
5	Iowa 2	42.45517	-90.6786	July, 2020
6	Wisconsin 1	43.112	-90.7066	July, 2020
7	Wisconsin 2	44.10483	-90.8402	July, 2020
8	Wisconsin 3	44.64364	-91.3084	July, 2020
9	Illinois 4	40.11962	-87.9631	July, 2021
10	Indiana 1	40.04634	-86.7499	July, 2021
11	Indiana 2	39.99172	-85.8628	July, 2021
12	Indiana 3	40.00483	-85.4401	July, 2021
13	Ohio 1	40.05559	-84.6591	July, 2021
14	Ohio 2	39.95099	-82.7309	July, 2021
15	West Virginia 1	40.05095	-80.68	July, 2021
16	Pennsylvania 1	40.16912	-80.2041	July, 2021
17	Pennsylvania 1	40.16586	-77.5982	July, 2021

Table 4.2 Reconstruction of the establishment of *D. radiella* across the USA and Canada with the use of literature and museum records.

State/Province	Date	Type	Record
Ontario	1862	Personal Observation	Bethune (1869)
Pennsylvania	1888	Collection Record	Collected by T Pergande, reported in Clarke (1941)
"Eastern United States"	1889	Personal Observation	Riley (1889)
Michigan	1890	Preserved Specimen	The Albert J. Cook Arthropod Research Collection
Illinois	1900	Collection Record	Collected by WD Kearfott, reported in Clarke (1941)
Quebec	1903	Collection Record	Collected by CH Young, reported in Clarke (1941)
Utah	1907	Collection Record	Collected by ESG Titus, reported in Clarke (1941)
Oregon	1914	Collection Record	Collected by L Leland, reported in Clarke (1941)
Nova Scotia	1915	Collection Record	No Collector Credited, reported in Clarke (1941)
Connecticut	1919	Preserved Specimen	The Yale Peabody Museum
Massachusetts	1920	Collection Record	Collected by JD Caffrey, reported in Clarke (1941)
Rhode Island	1920	Collection Record	No Collector Credited, reported in Clarke (1941)
Maine	1923	Preserved Specimen	The Yale Peabody Museum
Arizona	1925	Collection Record	Collected by OC Poling, reported in Clarke (1941)
British Columbia	1925	Collection Record	Collected by LE Marmont, reported in Clarke (1941)
Washington	1930	Collection Record	Collected by WW Baker, reported in Clarke (1941)
Indiana	1931	Collection Record	Collected by GS Walley, reported in Clarke (1941)
"All provinces of Canada"	1932	Personal Observation	Dustan (1932)
New York	1939	Collection Record	Collected by JFG Clarke, reported in Clarke (1941)
Minnesota	1947	Preserved Specimen	The University of Minnesota Insect Collection
Kentucky	1955	Collection Record	Evidence of webworm activity in herbarium sample, reported in Zangerl and Berenbaum (2005)
Ohio	1961	Preserved Specimen	The Cleveland Museum of Natural History Invertebrate Zoology Collection

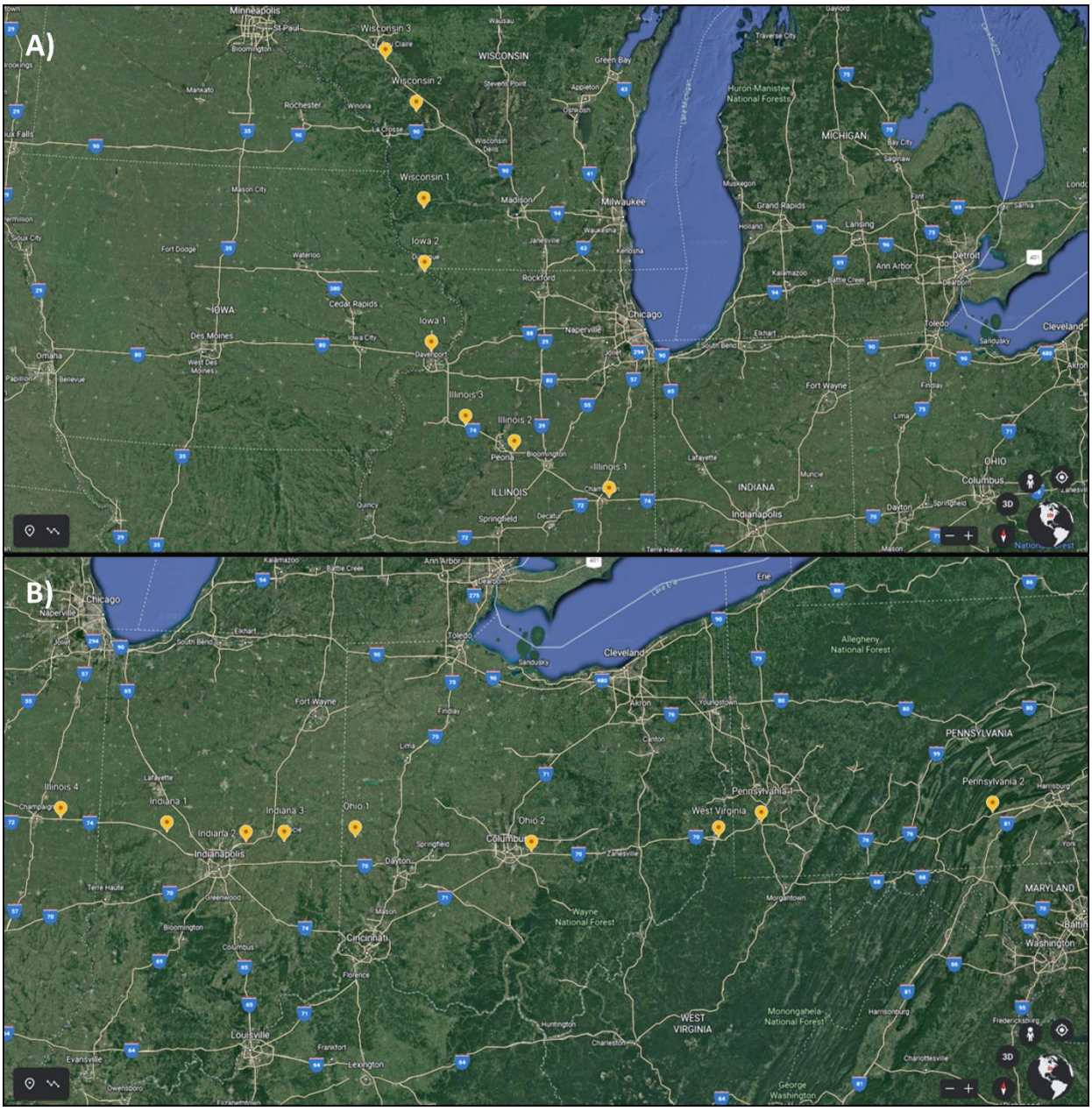

Figure 4.1 Maps depicting the sampling sites of both collection trips. A) 8 sites spanning across a latitudinal gradient from Urbana, IL to Eau Claire, WI (~680 km). B) 9 sites spanning across a longitudinal gradient from Urbana, IL to Newburg, PA (~1078 km).

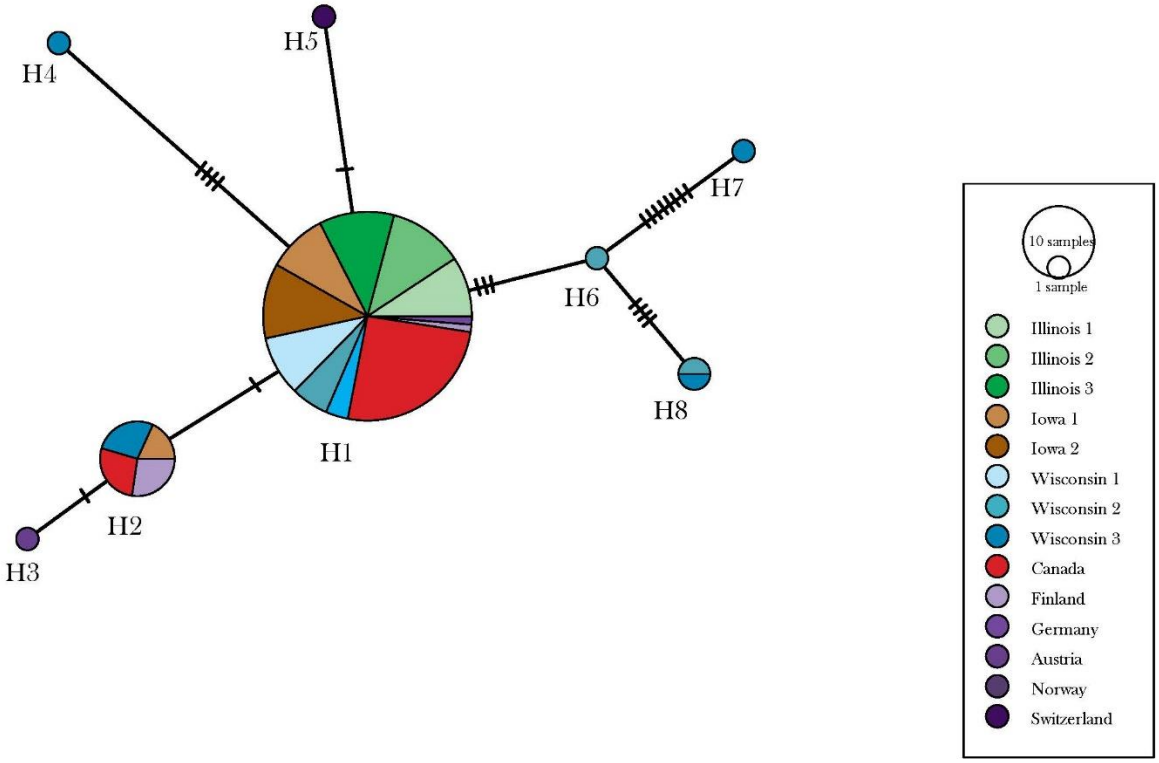

Figure 4.2 TCS (Templeton-Crandall-Sing) network depicting relationships between COI haplotypes of *Depressaria depressana* either collected from populations sampled along a latitudinal gradient from Urbana, IL to Eau Claire, WI or retrieved from the BOLD database. The size of each circle represents number of individuals belonging to each haplotype (H1- 7). The number of hash marks on branches between haplotypes represent the number of mutational steps.

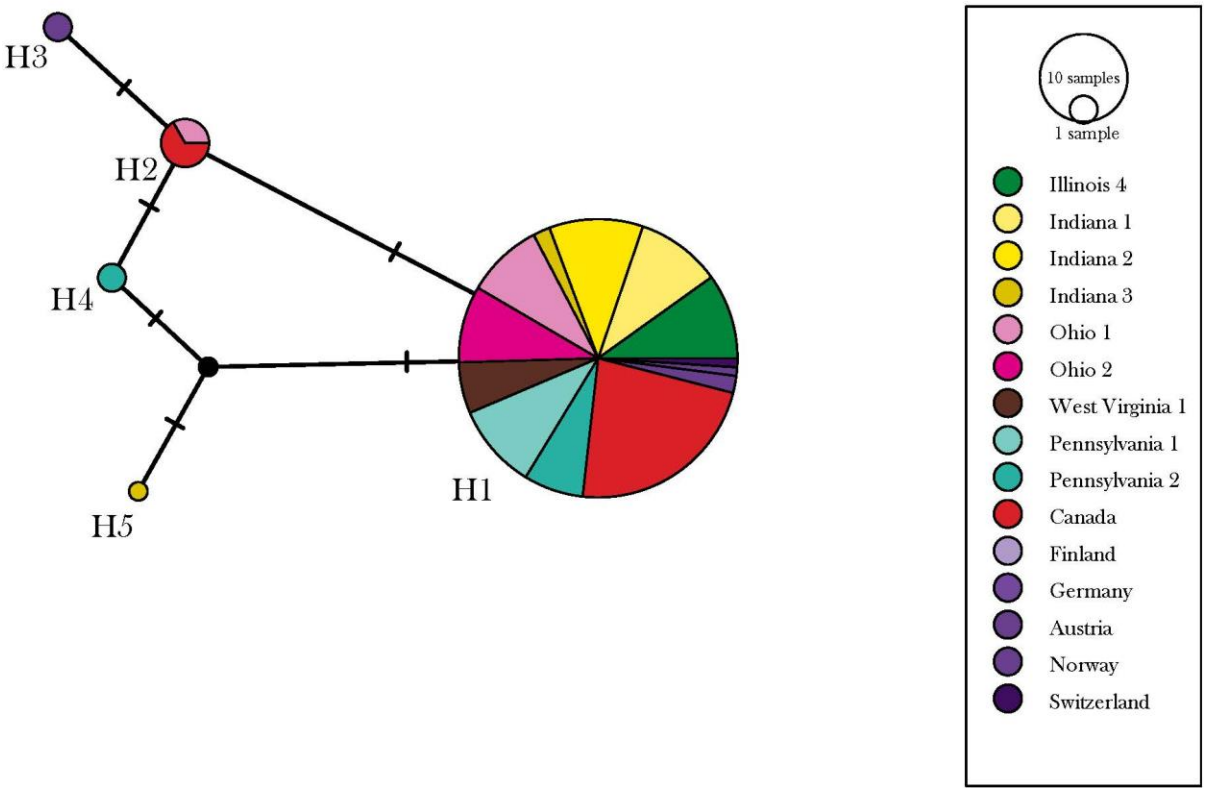

Figure 4.3 TCS (Templeton-Crandall-Sing) network depicting relationships between COI haplotypes of *D. depressana* either collected from populations sampled along a longitudinal gradient from Urbana, IL to Newburg, PA or retrieved from the BOLD database. The size of each circle represents number of individuals belonging to each haplotype (H1- 6). The number of hash marks on branches between haplotypes represent the number of mutational steps.

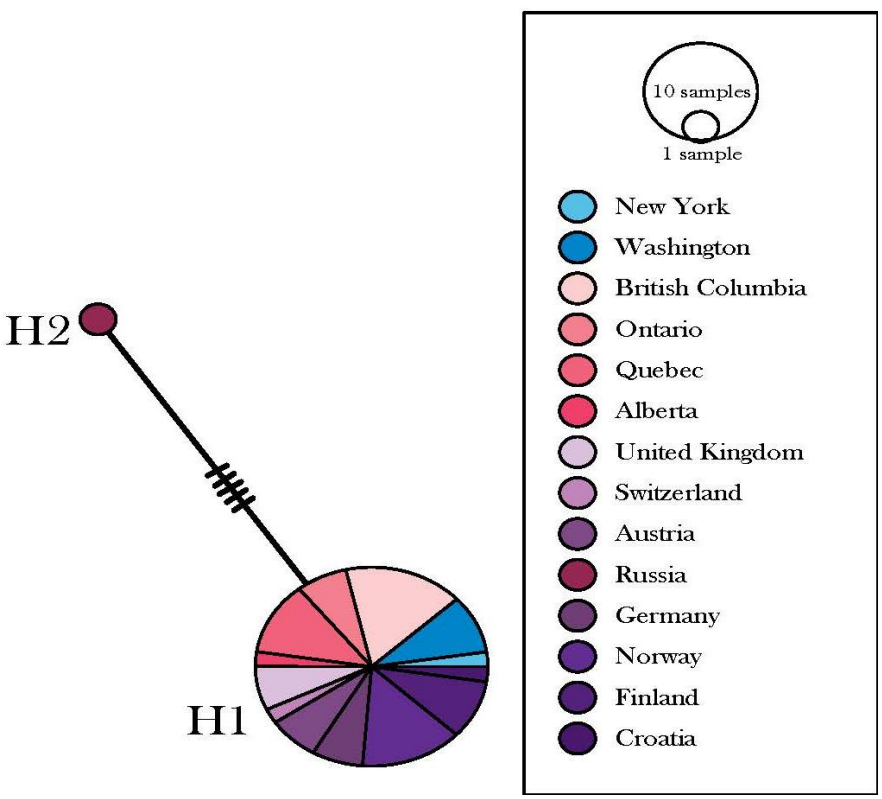

Figure 4.4 TCS (Templeton-Crandall-Sing) network depicting relationships between COI haplotypes of *D. radiella*. Partial COI sequences for all individuals in this analysis were retrieved from the BOLD database. The size of each circle represents number of individuals belonging to each haplotype (H1- 2). The number of hash marks on branches between haplotypes represent the number of mutational steps.

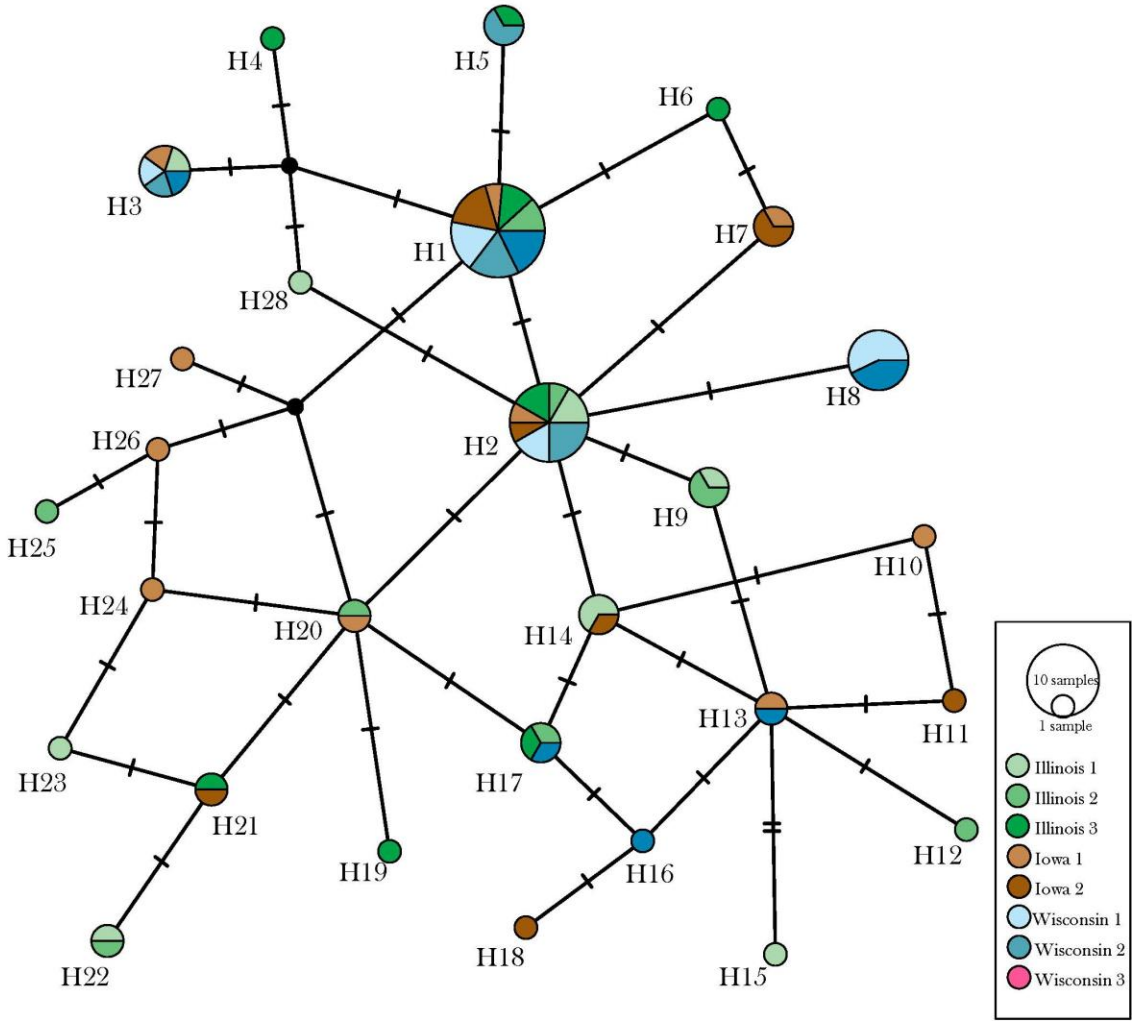

Figure 4.5 TCS (Templeton-Crandall-Sing) network depicting relationships between EF1α haplotypes of *D. depressana* either collected from populations sampled along a latitudinal gradient from Urbana, IL to Eau Claire, WI or retrieved from the BOLD database The size of each circle represents number of individuals belonging to each haplotype (H1-28). The number of hash marks on branches between haplotypes represent the number of mutational steps.

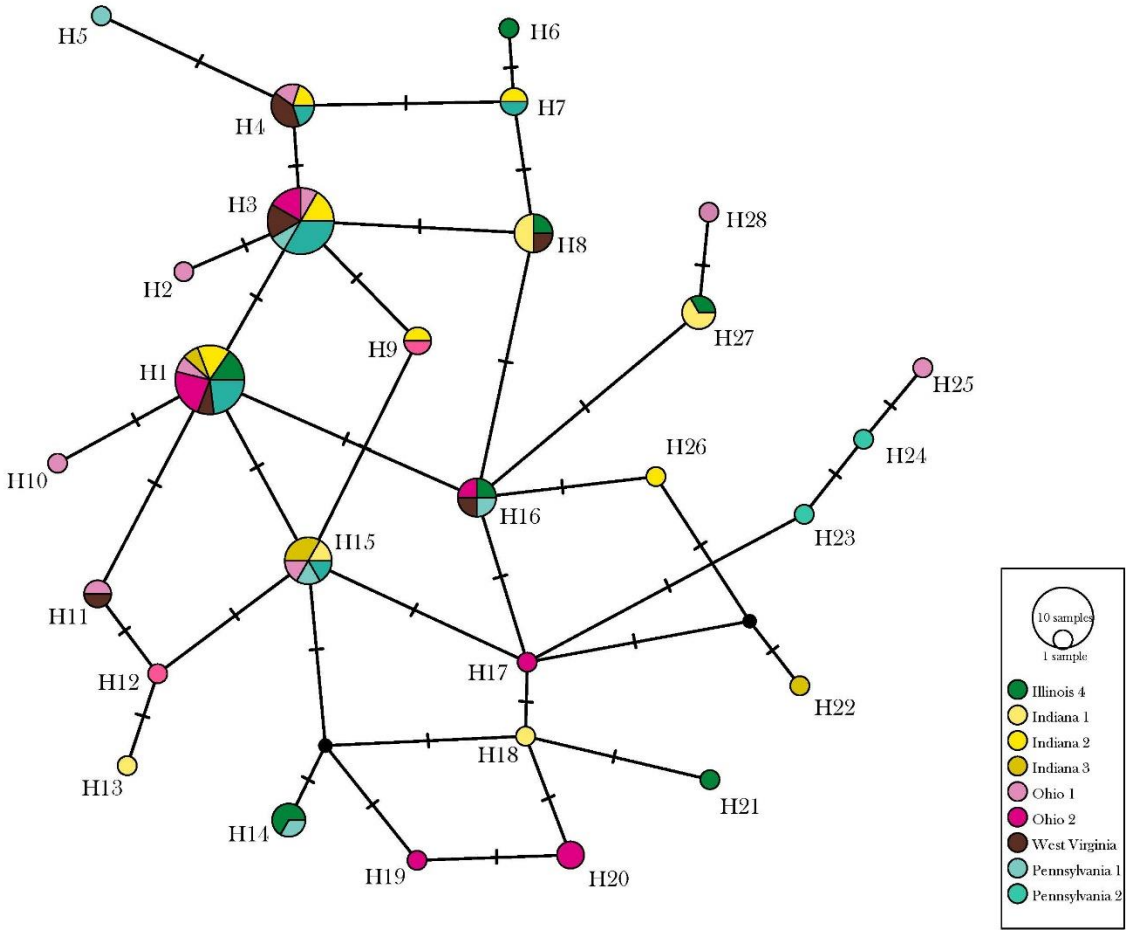

Figure 4.6 TCS (Templeton-Crandall-Sing) network depicting relationships between EF1α haplotypes of *D. depressana* either collected from populations sampled along a longitudinal gradient from Urbana, IL to Newburg, PA or retrieved from the BOLD database The size of each circle represents number of individuals belonging to each haplotype (H1-29). The number of hash marks on branches between haplotypes represent the number of mutational steps.

REFERENCES

Agrawal AA, Zhang X (2021) The evolution of coevolution in the study of species interactions. Evolution 75: 1594-1606.

Averill KM, DiTommaso A (2007) Wild parsnip (*Pastinaca sativa*): A troublesome species of increasing concern. Weed Technol 21: 279-287.

Balbi EI, Tosto DS, Flores FM, Arneodo JD (2020) Evidence for multiple maternal lineages of the invasive pest *Helicoverpa armigera* in Argentina. Phytoparasitica 48: 3.

Berenbaum MR (1981) Patterns of furanocoumarin distribution and insect herbivory in the Umbelliferae: plant chemistry and community structure. Ecology (62): 1254-1266.

Berenbaum MR (1983) Coumarins and caterpillars: a case for coevolution. Evolution 37: 163-179.

Berenbaum MR (1990) Evolution of specialization in insect-umbellifer associations. Ann Rev Entomol 35: 319-342.

Berenbaum MR (1991) Coumarins. In: Rosenthal G, Berenbaum MR (ed) Herbivores Their Interactions with Secondary Plant Metabolites. NY: Academic Press pp 221-249.

Berenbaum MR, Zangerl AR (1991) Acquisition of a native hostplant by an introduced oligophagous herbivore. Oikos 62:153-159.

Berenbaum MR, Zangerl AR (1992) Genetics of physiological and behavioral resistance to host furanocoumarins in the parsnip webworm. Evolution 46:1373-1384.

Berenbaum MR, Zangerl AR (1996). Phytochemical diversity: adaptation or random variation? In Phytochemical Diversity and Redundancy in Ecological Interactions (J. Romeo et al., eds) (pp. 1-24). Springer US.

Berenbaum MR, Zangerl AR, Nitao JK (1986) Constraints on chemical coevolution; Wild parsnips and the parsnip webworm. Evol 40: 1215-1228.

Bradshaw CJ, Leroy B, Bellard C, Roiz D, Albert C, Fournier A, Barbet-Massin M, Salles JM, Simard F, Courchamp F (2016) Massive yet grossly underestimated global costs of invasive insects. Nat Commun 7**:** 1-8.

Brower AVZ (1994) Rapid morphological radiation and convergence among races of the butterfly *Heliconius erato* inferred from patterns of mitochondrial DNA evolution. Proc Natl Acad Sci USA 91: 6491–6495.

Calla B, Wu WY, Dean CAE, Schuler MA, Berenbaum MR (2020) Substrate-specificity of cytochrome P450-mediated detoxification as an evolutionary strategy for specialization on furanocoumarin-containing hostplants: CYP6AE89 in parsnip webworms. Insect Mol Biol 29: 112–123.

Castalanelli MA, Cunningham RJ, Davis MB, Groth DM, Grimm M (2013) When genes go wild: highly variable internal transcribed spacer1 and conserved mitochondrial DNA haplotypes used to examine the genetic diversity and dispersal pathways of invasive *Hylotrupes bajulus* in Western Australia. Agric For Entomol 3: 236-244.

Caterino MS, Cho S, Sperling FA (2000) The current state of insect molecular systematics: a thriving Tower of Babel. Annu Rev Entomol 45: 1-54.

Cheng R, Jiang N, Yang X, Xue D, Liu S, Han H (2016) The influence of geological movements on the population differentiation of *Biston panterinaria* (Lepidoptera: Geometridae). J Biogeogr 43: 691-702.

Clement M, Posada D, Crandall KA (2000) TCS: A computer program to estimate gene genealogies. Mol Ecol 9: 1657–1659.

Dall ‘Acqua F, Vedaldi D, Recher M (1978) The photoreaction between furocoumarins and various DNA with different base compositions. Photochem Photobiol 27: 33-36.

Facon B, Genton BJ, Shykoff J, Jarne P, Estoup A, David P (2006) A general eco-evolutionary framework for understanding bioinvasions. Trends Ecol Evol?? 21: 130-135.

Finn DS, Theobald DM, BLACK IV WC, Poff NL (2006) Spatial population genetic structure and limited dispersal in a Rocky Mountain alpine stream insect. Mol Ecol 12: 3553-3566.

Harrison T, Dean CAE, Parks K, Berenbaum MR (2016) *Depressaria depressana* (Fabricius) (Depressariidae), new to the Midwestern USA. J Lepid Soc 70: 169–173.

Jogesh T, Zangerl A, Stanley M, Berenbaum M (2013) Implications of enemy escape on chemically mediated interactions with mutualists: wild parsnip pollination in two hemispheres. J Pollinat Ecol 11: 57-67.

Lee GS, Seo BY, Lee J, Kim H, Song JH, Lee W (2020) First report of the fall armyworm, *Spodoptera frugiperda* (Smith, 1797) (Lepidoptera, Noctuidae), a new migratory pest in Korea. Korean J Appl Entomol 2020;59(1):73-8.

Leigh JW, Bryant D (2015). PopART: Full-feature software for haplotype network construction. Methods Ecol Evol 6: 1110–1116.

Li J, Zhao F, Choi YS, Kim I (2006) Genetic variation in the diamondback moth, *Plutella xylostella* (Lepidoptera: Yponomeutidae) in China inferred from mitochondrial COI gene sequence. Eur J Entomol 103: 605-611.

Mack RN, Simberloff D, Lonsdale M, Evens H, Clout M, Bazzaz FA (2000) Biotic invasions: causes, epidemiology, global consequences, and control. Ecol Appl 10: 689-710.

McLaughlin GM, Dearden PK (2019) Invasive insects: management methods explored. J Insect Sci. 19: 1-9.

Nagoshi RN, Meagher RL, Hay-Roe M (2012) Inferring the annual migration patterns of fall armyworm (Lepidoptera: Noctuidae) in the United States from mitochondrial haplotypes. Ecol Evol 2:1458-1467.

Nagoshi RN, Rosas-García NM, Meagher RL, Fleischer SJ, Westbrook JK, Sappington TW, Hay-Roe M, Thomas JM, Murúa GM (2015) Haplotype profile comparisons between *Spodoptera frugiperda* (Lepidoptera: Noctuidae) populations from Mexico with those from Puerto Rico, South America, and the United States and their implications to migratory behavior. J Econ Entomol 108:135-144.

Palumbi SR (2001) Humans as the world's greatest evolutionary force. Science 293: 1786-1790.

Patrick BH (2004) Parsnip moth established in New Zealand. Weta 27: 8-12.

Peacock L, Worner SP (2008) Biological and ecological traits that assist establishment of alien invasive insects. N Z Plant Prot 61: 1-7.

Pysek P, Richardson DM (2010) Invasive species, environmental change and management, and health. Annu Rev Environ Resour 35: 25-55.

Schultheis AS, Weigt LA, Hendricks AC (2002) Gene flow, dispersal, and nested clade analysis among populations of the stonefly *Peltoperla tarteri* in the southern Appalachians. Mol Ecol 3: 317-327.

Snyder WE, Evans EW. Ecological effects of invasive arthropod generalist predators (2006) Annu Rev Ecol Evol Syst 37: 95-122.

van Nieukerken EJ, Doorenweerd C, Stokvis FR, Groenenberg DS (2012) DNA barcoding of the leaf-mining moth subgenus *Ectoedemia* s. str.(Lepidoptera: Nepticulidae) with COI and EF1-α: two are better than one in recognising cryptic species. Contrib Zool 81: 1-24.

Wang Y, Huang C, Hu B, Liu Y, Walter GH, Hereward JP (2020) Gene flow across host-associated populations of the rice stem borer *Chilo suppressalis* Walker (Lepidoptera: Crambidae): implications for Bt resistance management in rice. Pest Manag Sci 76: 695-703.

Zangerl AR, Berenbaum MR (2003) Phenotype matching in wild parsnip and parsnip webworms: causes and consequences. Evol 57: 806-815.

Zangerl AR, Berenbaum MR (2005) Increase in toxicity of an invasive weed after reassociation with its coevolved herbivore. Proc Natl Acad Sci USA 102:15529-15532.

Zangerl AR, Stanley MC, Berenbaum MR (2008) Selection for chemical trait remixing in an invasive weed after reassociation with a coevolved specialist. PNAS 12: 4547-52.